Published in final edited form as:
J Comp Neurol. 2011 February 1; 519(2): 211–237. doi:10.1002/cne.22513.

BRAIN EXPRESSION AND SONG REGULATION OF THE CHOLECYSTOKININ GENE IN THE ZEBRA FINCH (*TAENIOPYGIA GUTTATA*)

Peter V. Lovell and **Claudio V. Mello***
Institutional affiliations: Department of Behavioral Neuroscience, Oregon Health and Science University, 3181 Sam Jackson Park Rd L470, Portland, OR 97239, USA

Abstract

The gene encoding cholecystokinin (*Cck*) is abundantly expressed in the mammalian brain and has been associated with such functions as feeding termination and satiety, locomotion and self-stimulation, the modulation of anxiety-like behaviors, and learning and memory. Here we describe the brain expression and song regulation of *Cck* in the brain of the adult male zebra finch (*Taeniopygia guttata*), a songbird species. Using *in situ* hybridization, we demonstrate that *Cck* is highly expressed in several discrete brain regions, most prominently the caudal-most portion of the hippocampal formation, the caudodorsal nidopallial shelf and the caudomedial nidopallium (NCM), the core or shell regions of dorsal thalamic nuclei, dopaminergic cell groups in the mesencephalon and pons, the principal nucleus of the trigeminal nerve, and the dorsal raphe. *Cck* was largely absent in song control system, a group of nuclei required for vocal learning and song production in songbirds, though sparse labeling was detected throughout the striatum, including song nucleus area X. We also show that levels of *Cck* mRNA and the number of labeled cells increase in the NCM of males and females following auditory stimulation with conspecific song. Double labeling further reveals that the majority of *Cck* cells, excluding those in the reticular nucleus of the thalamus, are non-GABAergic. Together, these data provide the first comprehensive characterization of *Cck* expression in a songbird, and suggest a possible involvement of *Cck* regulation in important aspects of birdsong biology, such as perceptual processing, auditory memorization and/or vocal-motor control of song production.

Keywords

songbird; auditory; gene regulation; song learning; vocal control system

Introduction

Cholecystokinin (we use *Cck* for the mRNA and CCK for the peptide) was initially identified as a gut peptide that regulates the contraction of the gallbladder in response to gastric distension, but it is also one of the most abundant and widespread brain peptides, as revealed by immunohistochemical and *in situ* hybridization studies in several mammalian species (Ciofi and Tramu, 1990; Huntley and Jones, 1991; Ingram et al., 1989; Micevych et al., 1988). Consistent with its broad brain distribution, *Cck* has been implicated in a plethora of functions that are under the control of the central nervous system, ranging from feeding termination and satiety to the control of dopamine-mediated behaviors such as locomotion

*Corresponding Author: Claudio V. Mello, Department of Behavioral Neuroscience, Oregon Health and Science University, 3181 Sam Jackson Park Rd L470, Portland, OR 97239, USA.

and self-stimulation, the modulation of anxiety-like behaviors, and learning and memory. The major identified *Cck*-expressing cell types in the mammalian brain consist of a subpopulation of GABAergic neurons in cortical areas, the olfactory bulb, and hypothalamus, as well as dopaminergic neurons in the ventral tegmental area and in the substantia nigra (Doetsch et al., 1993; Fallon et al., 1983; Kawaguchi and Kubota, 1998; Kubota and Kawaguchi, 1997; Seroogy et al., 1988).

A previous study has examined the brain expression and regulation of *Cck* in one avian species, the chicken (*Gallus gallus*; Maekawa et al., 2007). That study identified *Cck* as a gene up-regulated in chick dorsal pallium, namely in the visual wulst and portions of the mesopallium, in the context of imprinting behavior and determined that *Cck*-expressing cells in these regions are mostly non-GABAergic, in an apparent contrast to mammals. The authors further demonstrated that intra-ventricular injections of davezepide, a potent CCK-receptor antagonist, prevented the acquisition of a novel visual imprinting stimulus. Thus, in chick, CCK signaling appears to play a prominent role in the acquisition of visual imprinting.

The brain-wide expression of *Cck* mRNA has not yet been described in any songbird species, though a recent study confirmed the presence of CCK (peptide and mRNA) in the adult zebra finch brain (Xie et al., 2010). Songbirds differ from the chicken in important ways with respect to brain and behavior, most conspicuously the fact that songbirds learn their vocalizations through reference to an auditory model (typically the song of the father or tutor) and possess a specialized set of forebrain vocal nuclei and projections known as the song control system (for reviews see Brenowitz et al., 1997; Zeigler and Marler, 2004; Zeigler and Marler, 2008). A schematic illustrating the connectivity of the song system in songbirds is presented in Fig. 1B. Ball et al., 1988 examined the localization of CCK by immunohistochemistry in the song system of two songbird species, the European starling (*Sturnus vulgaris*) and the song sparrow (*Melospiza melodia*), and found that it is expressed in cells within nucleus intercollicularis (ICo) including its dorsomedial nucleus (DM), which is part of the vocal-motor pathway in the song system. They also observed labeled fibers immediately ventrolateral to RA, possibly corresponding to a portion of the arcopallial cup area in the descending auditory pathway (Kelley and Nottebohm, 1979; Mello, 1998; Vates et al., 1996). Since these brain areas have been implicated in song learning and the auditory or motor control of song, these observations further raise the possibility that CCK might influence vocal learning and/or singing behavior.

Using microarrays, we recently identified *Cck* as a candidate differentially expressed gene in zebra finch brain (Lovell et al, 2008). Specifically, we found that *Cck* is relatively enriched in the nidopallial shelf (an auditory song-responsive region adjacent to song control nucleus HVC) in comparison to HVC, a key motor nucleus in the song system (Fig 1B). In a separate study (Lovell and Mello, unpublished observations) we have identified *Cck* as a candidate song-regulated gene in the caudomedial nidopallium (NCM), a higher-order auditory area implicated in song auditory processing and perceptual memorization (Mello, 1993; Hauber et al., 2007; Grace et al., 2003; Terleph et al., 2006; Terleph et al., 2007; Amin et al., 2004; Gobes and Bolhuis, 2007; Woolley and Doupe, 2008). In light of the role that elevated CCK levels play in the acquisition of visual imprinting in chicks, a behavior that is in principle analogous to song auditory memorization, the possibility that *Cck* might be regulated by song in NCM suggests an intriguing role for *Cck* in the auditory processing of birdsong.

Here we present a detailed characterization of *Cck* expression in the brain of the adult zebra finch using *in situ* hybridization. Our results indicate that *Cck* is distributed throughout the songbird brain, with strong expression in several subregions of the pallium. Though

expression was generally low in the song system, we detected expression in the shelf region beneath HVC, the cup region ventrolateral to the robust nucleus of the arcopallium (RA), and an anterior nidopallial region surrounding the lateral magnocellular nucleus of the anterior nidopallium (LMAN). We also detected sparse labeling throughout the striatum, including song nucleus area X, and confirmed previous reports of *Cck* expression in the midbrain's vocal nucleus DM. In NCM, we found that *Cck* expression was significantly induced by song auditory stimulation, and determined that both *Cck* mRNA expression levels and the number of *Cck*-expressing cells were significantly elevated in song-stimulated birds compared to unstimulated controls. We discuss these observations in the context of auditory song learning in birds, and in comparison with mammals, providing evidence for the conservation and divergence of various aspects of *Cck* brain expression among these vertebrate lineages.

MATERIALS AND METHODS

Birds and Song Stimulation

We used adult male and female zebra finches (*Taeniopygia guttata*) that were obtained from our own breeding colony or purchased from local breeders. For quantitative analysis of song stimulation experiments we primarily used females in order to avoid the confound of singing behavior in males. However, to address possible sex differences in the song-regulation of *Cck* we also conducted a similar analysis at a single time point after stimulation in males. Protocols for song presentation were essentially as in Velho et al., 2005. Briefly, birds were isolated overnight under 12:12-hour light-dark cycle (same as breeding aviary) in custom-built acoustic isolation chambers. The following morning (~10:00 AM) birds were either sacrificed without acoustic stimulation (i.e. control, unstimulated group; N = 5 females; N = 5 males) or presented with a 30 min playback of conspecific song (i.e. repeated medley of three unfamiliar zebra finch songs, each presented for 15 sec followed by 45 sec of silence, at 70 dB mean SPL at ~30 cm from the speaker). Females were sacrificed by decapitation 30 (N = 5), 90 (N = 6), or 240 min (N = 6) after the start of playback to produce three distinct song exposure groups. Song-stimulated males were sacrificed 30 min after the start of playback to produce a single song exposure group (N = 5). All animal protocols were approved by OHSU's IACUC committee and are in accordance with NIH guidelines.

Tissue Preparation

After decapitation brains were quickly removed, blocked in the coronal plane (for frontal sections) or along the midline (for parasagittal sections), and frozen in tissue-tek O.C.T. Compound (Sakura Finetek; Torrance, CA) in a dry ice/isopropanol bath, and stored at −80°C until sectioning. Parasagittal (10 μm) brain sections were cut on a cryostat, melted onto microscope slides (Superfrost plus; Fisher Scientific, Pittsburg, PA), and stored at −80°C for *in situ* hybridization.

Probe Preparation

Digoxygenin-(DIG)-, fluorescein- or ^{33}P-labeled riboprobes were synthesized using previously established protocols (Mello and Clayton, 1994; Velho et al., 2005). For clones from the ESTIMA zebra finch brain cDNA collection (http://titan.biotec.uiuc.edu/cgi-bin/ESTWebsite/estima_start?seqSet=songbird3), isolated plasmid DNA was restriction enzyme digested (BSSHII; New England Biolabs; Ipswich, MA) to release the insert template, and twice purified with Qiagen's PCR purification kit (Qiagen Inc., Valencia, CA). Plasmid containing a ~700 bp fragment of the zebra finch homologue of the 65-kDa isoform of glutamic acid decarboxylase (*Gad65*; Genbank accession AY364313; Pinaud et al., 2004) was also isolated, restriction enzyme digested and twice purified as for the ESTIMA clones. For both ESTIMA and PCR-derived templates,

sense and antisense strand probes were then synthesized at 37°C for 3–4 hours using the appropriate T3 or T7 RNA polymerase (Promega Inc., Madison, WI) and nucleotide label mix, purified by Sephadex G-50 columns, and for radioactive-labeled probes, quantified by a liquid scintillation counter (Beckman Coulter Inc., Fullerton, CA).

In Situ Hybridization

All of the methods for performing *in situ* hybridization were essentially as described previously (Mello and Clayton, 1994; Velho et al., 2005). Briefly, brain sections were post-fixed in a 3% buffered paraformaldehyde solution for 5 min at room temperature (RT), rinsed twice in 0.1 M PBS, and dehydrated through an alcohol series. Sections were then acetylated for 10 min in a solution of 1.35% triethanolamine and 0.25% acetic anhydride in water, and rinsed three times with 2x SSPE containing in mM: 300 NaCl, 20 NaH_2PO_4-H_2O, and 2.5 EDTA (pH 7.4). Each section was then hybridized with a solution (16 µl) containing 50% deionized formamide, 2x SSPE, 1 µg/µl tRNA, 1 µg/µl BSA, 1 µg/µl poly-A in DEPC-treated water, and 5×10^5 cpm of radioactively-labeled riboprobe or 1–2 µl of DIG- or fluorescein-labeled riboprobe. Slides were coverslipped, sealed by immersion in mineral oil, and incubated overnight at 65°C. The following day sections were rinsed in chloroform, de-coverslipped in 2x SSPE, and washed by incubating serially for 1 hr at RT in 2x SSPE, 1 hr at 65°C in 2x SSPE containing 50% formamide, and twice in 0.1x SSPE for 30 min at 65°C.

For radioactively-labeled probes, sections were then dehydrated in an alcohol series and analyzed by phosphorimager autoradiography with a low-energy screen and a Typhoon scanner (GE Healthcare, Piscataway, NJ) for densitometry.

For single-labeling non-radioactive *in situ* hybridization, sections were hybridized and washed as described above, then blocked for 30 min at RT in TNB buffer (100 mM Tris-HCl pH 7.4, 150 mM NaCl, 20 µg/µl bovine serum albumin, 0.3% Triton X-100), and then washed 3 times in TNT (100 mM Tris-HCl pH7.4, 150 mM NaCl, 0.3% Triton-X100). Sections were then incubated for 2 hr in TNB with an alkaline phosphatase conjugated anti-DIG antibody (anti-DIG-AP; 1:300 dil., Roche Applied Science, Mannheim, Germany), washed 3 times for 5 min in TNT, and incubated for 1–3 days in a ready-to-use tris-buffered solution containing the alkaline phosphatase substrates Nitro-Blue Tetrazolium Chloride (NBT; 0.42 g/L) and 5-Bromo-4-Chloro-3-Indolyl-phosphate p-Toluidine Salt (BCIP/NBT; 0.21 g/L; Substrate Solution NEL937, Perkin-Elmer, Waltham, MA). Slides were washed 3 times for 5 min at RT in TNT, rinsed briefly in distilled water to remove salts, and coverslipped with aquamount (Lerner Laboratories, Pittsburg, PA).

For single-labeling fluorescent *in situ* hybridization, sections were hybridized, washed, and blocked as described above, then incubated overnight at 4°C in TNB with a horseradish peroxidase conjugated anti-DIG antibody (anti-DIG-HRP; 1:1500 dil.; Roche Applied Science), washed 3 times for 5 min at RT in TNT, and then incubated at RT for 1 hr with Alexa 488-conjugated-tyramide in amplification buffer (1:100 dil.; Invitrogen, Carlsbad, CA) according to the manufacturer's recommended protocol. Slides were then washed 3 times for 5 min at RT in TNT, and coverslipped with aquamount.

For double-labeling fluorescent *in situ* hybridization (*Cck* with *Gad65*,), we used a DIG-labeled *Cck* riboprobe and a fluorescein-labeled *Gad65* riboprobe. Hybridizations, washes, and section blocking were conducted as described above for single-labeling fluorescent *in situs*. The DIG-labeled *Cck* probe was developed first using anti-DIG-HRP and Alexa-tyramide-488 as described above. Sections were then washed 3 times for 5 min in TNT, and incubated for 20 min at RT in TNT plus 0.2% HCl to inactive the anti-DIG-HRP followed by three washes for 5 min each in TNT. To visualize the fluorescein-labeled *Gad65* probe,

sections were then incubated for 2–4 hr in a solution of TNB with an HRP-conjugated anti-fluorescein antibody (1:800 dil., Roche Applied Science), washed 3 times for 5 min in TNT, incubated for 10 min at RT in a solution containing biotinylated-tyramide in manufacturer's amplification buffer (1:100 dil.; Invitrogen), washed 3 times for 5 min in TNT, incubated with alkaline phosphatase conjugated Streptavidin in TNB (1:1000 dil.; Perkin-Elmer), washed 3 times in TNT, and incubated for 1–4 hr with the alkaline phosphatase substrate ELF97 in ELF amplification buffer (1:20 dil.; ELF97 RNA *in situ* hybridization kit; Invitrogen) following the manufacturer's recommended protocol. Finally, sections were washed 3 times for 5 min in ELF wash buffer, counterstained with propidium iodide (0.1μg/mL in TNT), and coverslipped with ELF97 mounting medium.

For each set of double-labeling *in situs* we included additional negative controls slides that were incubated without one or the other primary antisera to confirm labeling specificity and to verify HRP inactivation. We also developed in parallel a set of single labeling *in situs* for the DIG- and fluorescein-labeled riboprobes to verify detection sensitivity.

Quantitative Analysis of *In situ* Hybridization Data

For all quantitative analyses, we first selected from each animal two adjacent parasagittal brain sections collected at ~1 mm from the midline. We confirmed brain level by examining cytoarchitectonic landmarks (position and shape of laminae and ventricular boundaries). Previous studies indicate that this level of NCM shows particularly complex gene expression and electrophysiological responses to song (Chew et al., 1995; Mello and Clayton, 1994; Ribeiro et al., 1998; Stripling et al., 1997). To assess the effect of song stimulation on *Cck* expression in NCM at this level we first performed optical density (OD) measurements on phosphorimager autoradiograms for sections processed for radioactive *in situ* hybridization. We used ImageJ software (NIH) to quantify levels of expression using the Gel-Data Linearization plug-in (http://rsb.info.nih.gov/ij/plugins/linearize-gel-data.html). For each bird we first measured the OD over the entire extent of NCM as contained in each section. The boundaries of NCM were defined as the region bounded dorsally, ventrally, and caudally by the ventricle, and rostrally by field L (Fig 1A; region 1). For each measurement, we then subtracted the tissue background, defined as the OD value measured over a portion of the white matter of the cerebellum, thus discounting any background due to non-specific stickiness of probe to the tissue and controlling for possible artifacts such as unevenness in the detection apparatus (phosphorimager screen). We next averaged these background-subtracted OD measurements from the two adjacent sections analyzed to obtain a single value per bird. Group differences in these background corrected values were compared by standard ANOVA model ($p < 0.05$), followed by *post hoc* t-tests (JMP7; SAS software; Cary, NC). To address the effect of song stimulation on the number of *Cck*-expressing neurons in NCM, we selected further parasagittal sections adjacent to those used for the OD measurements and processed them for fluorescent *in situ* hybridization for *Cck*. For each section we then mapped and counted all *Cck*-labeled cells within the boundaries of NCM (Fig 1A; region 1) or in a non-auditory region within the anterior striatum (Fig. 1A; region 2), using the Neurolucida/Lucivid system (Microbrightfield; Colchester, VT) integrated with a Nikon E-600 microscope equipped with a motorized stage drive and epifluorescence, We note that control measurements in the anterior striatum were performed in females, but not males to avoid the confound associated with the presence of striatal Area X in the latter. To account for any biases associated with counting cells in 10 μm thick brain sections, we re-estimated the total number of cells in each section by applying an Abercrombie correction (Abercrombie, 1946). Specifically, we measured the average diameter of 50 representative cells in NCM. We then adjusted our initial cell counts by multiplying each by a fixed Abercrombie correction factor as determined by [section thickness]/[section thickness*average cell thickness]. Since same-sized areas were counted in all birds, we refer

to a corrected cell number per section instead of cell density. In addition we did not perform a stereological analysis because our purpose was to estimate the relative change in the number of labeled cells in NCM as a result of stimulation rather than to derive exact counts of total labeled cells in NCM, as well as due to the intrinsic difficulties of performing stereology on the thin sections required for *in situ* analysis. We note that there is no evidence that cell density or the size of NCM might change as a result of our song stimulation paradigm. To test for any group differences in the number of labeled cells per NCM section as a function of song stimulation we used a standard ANOVA model ($p < 0.05$). If a significant effect was detected, *post hoc* pairwise t-tests were run to further characterize the effect of song stimulation. All statistical analyses were carried out using JMP8 (SAS Institute).

Image Acquisition and Figure Preparation

Images of non-radioactive *in situ* hybridization for *Cck* revealed with the NBT/BCIP chromogens (Fig. 3A and B) were acquired at 5X magnification using a high-resolution digital imaging system (3i Marianas System; Intelligent Imaging Innovations, Denver, CO) coupled to a Zeiss 200M microscope. Individual fields were acquired separately, flat field corrected, and then montaged in Slide-book 5.0 software. Additional higher power photomicrographs were acquired using bright-field, dark-field, or fluorescence optics and a Digital camera (DVC co., Austin, TX) coupled to a Nikon E600 microscope. For the schematic brain maps, we used the Neurolucida/Lucivid system (MBF Biosciences, Williston, VT) to map contours and major cytoarchitectonic landmarks, including laminae and boundaries of brain subdivisions and specific nuclei in a set of parasagittal Nissl-stained sections obtained from the same brains as used for the *in situ* hybridization analysis. We based our structure identification on available avian brain atlases, including the canary (Stokes et al., 1974), pigeon (Karten, 1966), chick (Puelles, 2007; Kuenzel, 1988), and zebra finch atlases (The Stereotaxic Atlas of the Brain of the Zebra Finch, Nixdorf-Bergweiler BE,), as well as previous publications on zebra finch neuroanatomy. We use the revised avian brain nomenclature (Reiner et al., 2004). Photoshop-CS2 (Adobe Systems Inc., San Jose, CA) was used to adjust photomicrographs. Specifically, we used the levels function to adjust the contrast and brightness of grayscale and color images. Color balancing was also performed across sections so that background levels were similar across brain sections. Figures were prepared in Illustrator-10 (Adobe Systems Inc.).

RESULTS

Identification of the Zebra Finch Ortholog of Cholecystokinin (*Cck*)

We identified a cDNA clone (GenBank EST accession CK302967) from the Songbird Neurogenomics Initiative consortium database (ESTIMA: Songbird3) that corresponds to the zebra finch ortholog of cholecystokinin (*Cck*). This transcript was identified as a candidate down-regulated marker of song nucleus HVC in a microarray comparison of mRNA expression in HVC versus the underlying nidopallial shelf region (Fig. 1B; see also Lovell et al., 2008). Further searches of ESTIMA: Songbird and the Songbird Brain Transcriptome database (http://songbirdtranscriptome.net) revealed 10 ESTs that corresponded to at least three distinct mRNA variants of *Cck* (Fig. 2A; var1–3) These variants differed with respect to the overall length of their 3’ untranslated regions (3’-UTR) as bioinformatically established by presence of a predicted polyadenylation tag, with the longest variant (var3) being 423 bp longer than the shortest (var1). Despite differences in the lengths of 3’-UTR, the variants were 100% identical within the predicted coding domain and in the overlapping non-coding regions. The *in situ* hybridization data presented here were derived from probes synthesized from the shortest *Cck* var1 (clone CK302967), however

similar results were obtained using probes derived from the longest clone (var3; DV961733; Fig. 3A–B).

The zebra finch *Cck* gene consists of three exons that span a ~7 kb region of chromosome 2 with the largest open reading frame starting in the 2nd exon. Based on an analysis of the predicted amino acid sequence (Fig. 2B), the unprocessed zebra finch CCK pre-prohormone is 130 amino acid in length, and shows 83.3%, 50.8% and 50.8% identity at the amino acid level with chicken, mouse, and human, respectively. The relatively low conservation between the full-length mammalian and avian pre-prohormones is due to several single or double amino-acid insertions, a 9 amino-acid insertion at position 22–30 in avian orthologs, and several non-conservative amino-acid substitutions. However, the peptide sequences within restricted regions corresponding to known post-translational endoproteolytic peptide products CCK-58, CCK-39, CCK-33, and CCK-22 (Fig. 3B; arrowheads indicate peptide cleavage sites that give rise to these products; arrowhead indicates the position of the carboxy-terminus in the mature peptide) were progressively more similar to mammalian orthologs. The shortest moiety, CCK-8 (residues 110–118), which is also the most prominent molecular form of the CCK peptide in the brain of most species, was 100% conserved across birds and mammals and includes a tyrosine residue at position 2 (indicated in Fig. 2B by an asterisk) that is typically sulfated to facilitate proper interactions with CCK receptors (Bodanszky et al., 1978).

To confirm the specificity of *Cck* labeling by *in situ* hybridization we conducted hybridizations using sense versus antisense strand riboprobes derived from two transcript variants of *Cck* (Fig. 2A; var3; CK302967 and var1; CK314171). Hybridizations with antisense probes gave identical expression patterns and cellular labeling (Fig. 3A, B), whereas hybridization with sense strand probes under the same conditions did not yield detectable signal (Fig. 3C, D). We note that although partially overlapping, var3 contains a unique stretch of ~423 bp at its 3'UTR, corresponding to ~40% of the typical length for our riboprobes as determined by agarose gel electrophoresis. Since we use high stringency *in situ* hybridization conditions (i.e., low salt and high hybridization and wash temperatures) we expect the probes for the two variants above to show specificity towards their respective transcripts, yet there was no observable difference in their hybridization patterns.

Cck Expression: Global Brain Distribution of mRNA

We observed that *Cck*-expressing cells are widely distributed throughout the brain of adult male zebra finches (Fig. 4) in a pattern qualitatively consistent across animals (N = 4) and similar to that seen in females (not shown). In general, labeled areas had a low to moderate density of *Cck*-expressing cells, although some discrete regions showed a high density of cells with high levels of *Cck* expression, yielding an overall patchy pattern. Areas with marked expression that could be visualized in low magnification views included the medial portions of the intermediate nidopallium and hyperpallium, the dorsolateral pallium, the caudal part of the hippocampal formation and parts of the dorsal thalamus, midbrain and pons. We note that fiber tracts and commissures, the ventricular region, the meninges and the choroid plexus were devoid of labeled cells, suggesting that *Cck* is primarily expressed in neurons and not vascular tissue, glia, or ependymal cells. We describe below the expression patterns observed according to brain region, based primarily on examination of parasagittal sections in males. These observations are consistent with the pattern observed in females. We note, however, that since the song system is largely lacking or reduced in females, comments concerning labeling in and around song nuclei refer primarily to males. A summary of the regions examined and their relative expression of *Cck* is presented in Table 2.

Cck Expression: Telencephalon

The distribution of labeled cells throughout pallial subdivisions was not uniform, but rather seemed to define subregions that differed in terms of the density and labeling intensities of *Cck*-expressing cells. Starting with medial levels, we observed that the rostral hyperpallium had a high density of labeled cells with moderate to strong labeling (Fig. 4A–B). More caudally, starting at the rostral tip of the lateral ventricle (Fig. 4A–B, arrow) we observed an abrupt interruption in the labeling, and the parahippocampal (APH) region was mostly devoid of labeled cells. Similarly, labeled cells were lacking in a triangular-shaped area at the rostral-most end of the hyperpallium (Fig 4A,B, asterisk) that may correspond to anterior olfactory areas based on comparisons with the chicken brain atlas. At more lateral levels (Fig. 4C–F), the labeling intensities of hyperpallial cells became weaker and labeled cells less frequent. Although we did not attempt to distinguish among hyperpallial subdivisions, the predominance of labeled cells at medial levels suggests that most expression occurs within the medial apical hyperpallium.

At even more lateral levels (Fig. 4G–I), we observed a narrow dorsal band containing a high density of strongly labeled cells, underneath the brain surface (Fig 4G–I). This band became increasingly thicker more laterally and had a sharp boundary rostrally. This field seems to be continuous with a thinner rim of labeled cells underneath the pial surface along the whole extent of the dorsolateral and ventrolateral telencephalon as seen most easily in frontal sections (Fig. 5A–C). Based on this localization and in comparison with the chick and pigeon atlas, we conclude that this band encompasses the external portion of the dorsolateral corticoid area (Fig. 5B) and the piriform cortex (Fig. 5C).

We also observed a high density of strongly labeled cells in the caudal portion of the hippocampal formation (Figs. 4B–D and 6B), within a region located between the dorsocaudal nidopallium and the cerebellum. The *Cck*-expressing cells were confined to the cell-rich central domain of this region, and absent from the fiber-richer bands adjacent to the ventricle and pial surfaces (Fig. 6B). Cells were also absent from the caudoventral most portion of the hippocampal formation, a narrow domain located between the ventricle and the cerebellum that tapers off ventrally.

Rostral to the caudal hippocampal region, the APH was largely devoid of cells. Immediately beneath the APH we observed a narrow band of labeled cells (indicated by arrows in Fig. 6C–D). This band was adjacent to but respected the ventricular zone, which was clearly devoid of labeled cells, and likely corresponds to the periventricular stratum defined in the chick atlas. The band extended over a broad medial-to-lateral range (Fig. 4B–E), and was mirrored by a thin band of strongly labeled cells in the dorsal caudal mesopallium (CM) on the ventral side of the ventricular zone (indicated by arrowheads in Fig. 6C–D). Except for this caudodorsal band and for a few labeled cells scattered in its rostromedial portion, the mesopallium was mostly devoid of labeled cells.

The nidopallium had some of the highest *Cck* labeling intensity, particularly within its intermediate region, rostral to field L and caudal to song nucleus MAN (both medial and lateral subdivisions; Fig. 4A–E). Here we observed some cells with very high labeling intensity interspersed among a large number of cells with relatively low labeling intensities, suggesting the occurrence of distinct cell populations (Fig. 7B). Despite this apparent difference, the majority of labeled cells in the nidopallium were of similar small size and shape (Fig. 7C). Although this labeling pattern could be seen over a wide medial-to-lateral range, the strongly labeled cells became scarcer and overall cell labeling intensities weaker at lateral brain levels (Fig. 4F and G). A comparable pattern was seen in the rostral nidopallium, although song nucleus MAN and its surroundings were conspicuously devoid of labeled cells (Fig. 4D and E). The caudomedial nidopallium (NCM) had a moderate

number of cells with intermediate labeling intensities in its rostral portion, whereas the more caudal region was devoid of labeled cells (Fig. 4B and C). All field L subdivisions were negative for *Cck*.

Laterally, we observed a large number of labeled cells within the auditory nidopallial shelf region ventral to HVC (Fig. 4D–G and 7D). These labeled cells seemed to form a continuum with the labeled cells in the periventricular stratum of dorsal CM (Fig. 4D–G), the labeling being most pronounced in the intermediate and rostral shelf (Fig. 7D). In contrast, labeled cells were conspicuously absent within song nucleus HVC (Fig. 4D–G and 7D), and in another nidopallial song control area, the nucleus interfacialis.

Within the arcopallium, labeled cells were seen in an arc-like domain located beneath the dorsal arcopallial boundary (Fig. 4G–I), but were practically absent from other arcopallial regions including song nucleus RA and the adjacent cup region.

Among sub-pallial regions, the medial striatum contained strongly labeled cells that were sparsely and evenly distributed (Fig. 4A–G). We observed a similar pattern within song nucleus area X (Fig. 7E), wherein *Cck* was strongly expressed in sparse and evenly distributed populations of relatively large neurons (Fig. 7F), and smaller cells (Fig. 7G). Much fewer labeled cells were evident in the lateral striatum (Fig. 4H and I). In contrast, the globus pallidus, ventral pallidum and the septal region were essentially devoid of labeled cells.

Cck Expression: Diencephalon

The dorsal thalamus was one of the regions containing the highest density of labeled cells and cells with the highest labeling. The labeled cells partially or completely surrounded the nuclei such as dorsomedial nucleus of the anterior thalamus and the medial portion of the dorsolateral nucleus of the thalamus, forming shell-like domains around negative cores (Figs. 4B–D). Such a pattern was particularly evident in frontal sections at the level of the dorsomedial nucleus of the anterior thalamus (Fig. 8B). We also observed a high density of highly labeled cells immediately caudodorsal to auditory nucleus ovoidalis (Ov), corresponding to a portion of the Ovshell (Vates et al., 1996); the Ovcore was mostly devoid of labeled cells (Fig. 8C). The visual nucleus rotundus (Rt) contained in its core a large number of labeled and large cells that were clearly evident in both sagittal (Fig. 4E–F) and frontal sections (Fig. 8D). In contrast, both the medial and lateral habenula were entirely negative for *Cck* (Fig. 4A–C).

Cck Expression: Mesencephalon and Metencephalon

We observed a large number of labeled cells within the ventral tegmental area (VTA) immediately caudodorsal to the oculomotor nucleus (NIII; Figs. 4B and 9B), as well as strong labeling in an area immediately rostral to the isthmooptic nucleus (IsO) that based on the chick atlas likely corresponds to dopaminergic cell group A11 (Figs. 4D and 9D). We also detected sparse labeling throughout a region rostral to A11 corresponding to the substantia nigra pars reticulata (SNr; Fig. 9E).

We observed strongly labeled cells in a discrete and distinct nucleus immediately caudal to the nucleus of the trochlear nerve (Fig. 10A’), corresponding to the dorsal raphe nucleus of the midbrain. We also detected labeling in a nucleus ventral to the dorsal raphe that based on the relative position and in comparison to the chick atlas, corresponds to the ventral median portion of the raphe (Fig. 10B’). Within the midbrain’s intercollicular nucleus (ICo), we observed moderate *Cck*-labeling that was primarily restricted to the regions immediately surrounding the dorsal medial nucleus of the ICo (DM) and nucleus mesencephalicus

lateralis, pars dorsalis (MLd; Fig. 10C'), in a shell-like fashion. In contrast, the optic tectum was for the most part devoid of labeling (Fig. 4G–I).

In the pons, the principal nucleus of the trigeminal nerve contained numerous labeled cells and could be clearly defined by their distribution (Figs. 4D–E and 10D'). In contrast, the cerebellum, including the cortical region and deep nuclei, was distinctly devoid of labeling.

Characterization of *Cck*-Expressing Cells in the Songbird Brain

Previous studies have shown that the majority of *Cck*-expressing cells in the mammalian cortex, hippocampus, and dentate gyrus are GABAergic interneurons, characterized by the co-expression of the GABAergic marker glutamic acid decarboxylase 65 (*Gad65*, Jinno and Kosaka, 2003; Kawaguchi and Kondo, 2002; Klausberger et al., 2005; Somogyi et al., 1984). In contrast, *Cck*-expressing cells in the pallium of the chick appear to be largely glutamatergic, co-localizing instead with the vesicular glutamate transporter *Vglut2* (Maekawa et al., 2007). To investigate the neurochemical phenotype of *Cck* cells in the songbird brain, we conducted double *in situ* hybridization for *Cck* and *Gad65*. As expected, based on previous observations in the zebra finch (Pinaud et al., 2004), *Gad65*-expressing cells were widely scattered throughout the pallium, including NCM, and highly enriched within the striatum. Despite this, we did not observe evidence of significant cellular co-localization of *Cck* and *Gad65* in the majority of pallial and sub-pallial brain areas surveyed (see example in Fig. 11A–C), indicating that most *Cck*-expressing cells in the zebra finch brain are non-GABAergic. In stark contrast, within the reticular nucleus of the thalamus (identified based on its position dorsal to Rt and in comparison with the chick atlas), virtually all *Cck*-expressing cells co-expressed *Gad65*, indicating that they are GABAergic (Fig. 11D–F; arrowheads indicate examples of double-labeled cells). This, however, appeared to be the only prominent avian brain structure where such a co-localization was evident.

Song regulation of *Cck* in NCM

Cck was previously detected as a candidate song-induced gene in a microarray screening (Lovell and Mello, unpubl obs). We therefore decided to directly investigate whether *Cck* is regulated by song in NCM by comparing *Cck* expression in the NCM of unstimulated controls (N = 5) versus birds sacrificed at 30 (N = 6), 90 (N = 5), and 240 min (N = 5) after the start of a 30 min song stimulation period (Fig. 12A). We conducted this analysis in females to avoid a potential confound of singing behavior in males, so that the possible gene regulation could be unequivocally linked to song auditory stimulation (see Materials and Methods). We performed optical densitometry (OD) measurements over the entire NCM area that is contained within a parasagittal section (region 1 in Fig. 1A) from a set of phosphorimager autoradiograms resulting from a radioactive *in situ* hybridization for *Cck*. We note that this level of NCM corresponds to a lateral portion that has previously been shown to exhibit complex genomic and electrophysiological responses to song stimulation (Chew et al., 1995;Mello and Clayton, 1994;Stripling et al., 1997;Ribeiro et al., 1998). The results revealed a significant effect of song-stimulation on *Cck* expression over NCM (Fig. 12B, top graph; ANOVA, $p = 0.0015$), with mRNA levels rising ~30 min after the start of song-stimulation and remaining elevated for up to 4 hr after the start of song presentation. We did not address any time points beyond 4 hours in our study. A *post hoc* analysis revealed that the effect of song-stimulation was significant at all time points relative to controls ($p = 0.0017$, 0.003 and 0.0004 for 30, 90, and 240 min, respectively). To further characterize this effect, we performed a fluorescent *in situ* hybridization analysis in a set of sections adjacent to those used for the autoradiographic analysis, and counted the number of labeled cells over the entire extent of NCM present in the brain sections analyzed (Fig. 12B, bottom graph and 12C; for measurement details see Materials and Methods). We also

performed a comparable non-fluorescent *in situ* hybridization in a set of control (N = 5) and song-stimulated (30 min; N = 4) males to address any sex differences in the regulation of *Cck* by song. We found a significant effect of song on the number of *Cck*-expressing cells in both males (t-test; t = 3.2; N = 9; $p < 0.01$) and females (ANOVA; F = 5.2; N = 21; $p < 0.01$), with the number of cells in females peaking 240 min after the onset of song presentation. In males we did not address time points beyond 30 min. Protected t-tests confirmed that the effect of song-stimulation was significant in females at all time-points relative to the controls (Fig. 12B black bars; p = 0.0098, 0.0328 and 0.0015 for 30, 90, and 240 min, respectively). In contrast, counts of *Cck*-positive cells in females over a 1 mm^2 region of the medial striatum that is not associated with the avian auditory system was unchanged with song presentation (Fig. 12B white bars; ANOVA; F = 0.14; p = 0.93). We note that there were no apparent increases in the number of labeled cells over other auditory areas including CMM and adjacent field L subdivisions (Fig. 12C); in fact these areas continued to be devoid of labeled cells even after song stimulation. Together these results indicate that the overall expression levels of *Cck* transcript as well as the number of *Cck*-expressing neurons undergo significant and sustained increases with song presentation, and that this effect is specific to auditory NCM.

Discussion

We have used *in situ* hybridization to characterize the expression of the *Cck* gene in the brain of the zebra finch (*Taeniopygia guttata*), a songbird species. We observed that *Cck* mRNA is highly expressed in several distinct brain regions, including the caudal portion of the hippocampal formation, discrete domains within the nidopallium, mesopallium and arcopallium, the core and/or shell regions of many thalamic nuclei, as well as a few other discrete brainstem nuclei. Moreover, consistent with a previous report in chicks but contrary to the data from mammals, virtually all of the *Cck*-expressing cells in the zebra finch pallium appear to be non-GABAergic. Lastly, our study provides confirmatory *in* situ evidence for previous microarray findings of differentially lower expression of *Cck* in song nucleus HVC of adult males in comparison to the nidopallial shelf (Lovell et al., 2008), and for an induction of *Cck* in NCM in response to auditory stimulation with conspecific song.

The *Cck* expression patterns we observed help define some pallial subregions that are not easily identifiable based on cytoarchitectonic criteria or the expression of previously characterized genes. Examples include intermediate, caudal and dorsal portions of the nidopallium, the rostromedial hyperpallium, and the caudal hippocampus, all defined by strong *Cck* expression. We discuss below the comparative and functional implications of our findings.

Of note, despite early studies of *Cck* in the mammalian brain suggesting discrepancies between the distribution of *Cck* mRNA and peptide (mRNA: Ingram et al., 1989; Voigt and Uhl, 1988; Burgunder and Young, 1988; Peptide: Miceli et al., 1987; Fallon and Seroogy, 1984), more recent studies using higher concentrations of colchicine and alternate methods of tissue fixation have largely confirmed overlapping distributions (Ogawa et al., 1989; Fox et al., 1991; Meziane et al., 1997; Morino et al., 1994). However, since we have not specifically examined CCK peptide in the zebra finch brain, it is important to keep in mind that any interpretations concerning peptide distribution based on based on mRNA should be taken with caution.

Cck expression: comparison with other birds

Maekawa et al., (2007) used very similar *in situ* hybridization techniques (i.e. DIG-probes and chromagen precipitation) as in our current study to map the distribution of *Cck* mRNA in frontal brain sections of the chick. As far as we are aware that report is the only published

study on the brain expression of *Cck* mRNA in an avian species. While the patterns of *Cck* expression are similar when comparing the telencephali of zebra finch and chick, we also note some significant differences. In chick, *Cck* is strongly expressed throughout the dorsal pallium, particularly the mesopallium (dorsal and ventral), hyperpallium (intercalatum) and area parahippocampalis, but is relatively weak or absent within the rostral, intermediate, and caudal nidopallium. In contrast, in zebra finch, we detected the strongest expression in the intermediate and caudal nidopallium, and little to no expression in the dorsal pallium with the exception of the periventricular stratum. While these differences could reflect differences in the functional role of *Cck*, we cannot discard an effect due to developmental ages.

In chick, prior to post-hatch day 6, levels of *Cck* and the immediate early gene *c-fos* increase significantly in the dorsal pallium following the presentation of visual stimuli, suggesting that the expression of *Cck* in the dorsal pallium might be important for the acquisition of visual imprinting (Maekawa et al, 2007). Maekawa et al corroborated that hypothesis by demonstrating that injections of devazepide, an antagonist of the brain form of the CCK receptor, greatly diminishes a chick's preference for imprinted visual objects. We have shown here that *Cck* (both levels and numbers of labeled cells) increase rapidly in zebra finch NCM (both sexes) in response to song presentation. Previous studies using song-inducible gene expression (*zenk*, *arc*, *c-jun*) and electrophysiology indicate that NCM plays an important role in birdsong perceptual processing and discrimination, as well as in aspects of the auditory memorization of birdsong (for reviews see Bolhuis and Eda-Fujiwara, 2003; Bolhuis et al., 2001; Mello et al., 2004; London and Clayton, 2008). The parallels in *Cck* inducibility by different modalities in the context of sensory learning raise the intriguing possibility that *Cck* function in birds is related to the acquisition of new sensory memories. Moreover, the *Cck* induction in different brain regions is more likely to reflect an activation of specific sensory modalities (e.g. vision or audition) as opposed to a species difference in function.

Maekawa et al (2007) also report that the *Cck* neurons within the pallium and subpallium are predominantly glutamatergic, as judged by their cellular co-expression with the glutamate transporter, VGLUT2. Since a VGLUT2 probe is currently not available in songbirds, we chose to address the neurochemical identity of *Cck* neurons in songbirds by double labeling for the GABAergic cell-type marker *Gad65*. Consistent with chick, we found that the vast majority of *Cck*-expressing cells in the zebra finch brain are non-GABAergic as judged by their lack of co-localization with *Gad65*. Taken together, these observations argue that *Cck*-expressing cells in the avian brain are mostly glutamatergic in nature. It will be intriguing to investigate further when this marked dichotomy between birds and mammals arose during evolution.

In contrast to other brain areas, virtually all the *Cck*-labeled cells within the thalamic reticular nucleus, an area not considered in the chick study, co-express *Gad65* and can thus be considered GABAergic. While the functional implications of this specialization are not immediately clear, it indicates that different avian brain regions can differ substantially with respect to the phenotype of their *Cck*-expressing cells.

Cck expression: comparison with mammals

Our data point to significant parallels but also several significant discrepancies in the brain distribution of *Cck* mRNA between mammals and the zebra finch. We discuss below our data in comparison with the mouse, since detailed expression data are available through the Allen Brain Atlas (Lein et al., 2007; Ng et al., 2009), and these data are largely in agreement with previous *in situ* hybridization studies (e.g. Savasta et al., 1989; Schiffmann and Vanderhaeghen, 1991). We note that while the general distribution of *Cck* is similar across

various mammals, particularly in the neocortex, some species differences in the ventral forebrain, thalamus, and hypothalamus have been reported and are considered below when relevant. We also note, that while it has been recently recognized that the avian telencephalon is more similar to the mammalian telencephalon than previously thought, including a clear distinction between pallial and basal ganglia regions, the homology of specific areas such as the derivatives of the avian dorsal ventricular ridge to specific mammalian pallial areas is still contentious (Jarvis et al., 2005; Reiner et al., 2004). Similarly, the avian equivalents of areas such as cortical layers, amygdalar subregions, endopiriform nucleus and claustrum are still largely unclear. Despite these limitations, some apparently conserved features of *Cck* expression present themselves.

In the mouse, pyramidal neurons in hippocampal CA1 and CA3 fields within Ammon's horn show strong *Cck* labeling, however little signal is detectable within the dentate gyrus with the exception of a few cells within the polymorph layer (Schiffmann and Vanderhaeghen, 1991). In the zebra finch, we have observed strongly labeled cells restricted to a caudal domain within the hippocampal formation (HF) on parasagittal sections at ~0.5 – 1.4 mm from the mid-line (Fig 4B–D, 6B), but not in any other HF domains, including the very caudal ventral strip between the ventricle and cerebellum and the area parahippocampalis. This pattern appears to be consistent with the CCK-like immunoreactivity in the pigeon HF, consisting of baskets surrounding a v-shaped region of large pyramidal cells that resemble the pyramidal cells of Ammon's Horn in mammals (Erichsen et al., 1991). We therefore suggest that the labeled region in the zebra finch HF likely corresponds to Ammon's Horn, with the caudal ventral strip corresponding to the dentate gyrus. We note, however, that the organization of the avian HF is still controversial, and that many recent studies that have addressed this structure have been conducted in frontal sections, making direct comparisons with our current data difficult (Atoji and Wild, 2006; Erichsen et al., 1991; Krebs et al., 1991; Szekely and Krebs, 1996). While precise homologies at the level of hippocampal subdivisions remain to be worked out, our data point to a specific feature (i.e. *Cck* expression in CA fields and their presumed avian counterparts) that seems conserved between mammals and birds. Based on lesion studies, it is generally thought that the hippocampus in birds serves a similar function as in mammals, namely the acquisition and representation of landmark cues that can be used to guide navigation (Gagliardo et al., 1999; Vargas et al., 2004; Watanabe, 2001). Of note, a recent lesion study in the hippocampus of the zebra finch has confirmed that the avian HF is involved in spatial memory function, but not song learning, singing or song structure (Bailey et al., 2009).

Another prominent feature of the mammalian brain is that the supragranular and infragranular layers of the sensory, motor and association cortices (i.e. cortical layers II–III and V–VI, respectively) exhibit strong *Cck* labeling, whereas the thalamorecipient layer (i.e. layer IV) is virtually devoid of *Cck* cells. Based on their connectivity, the avian primary thalamo-recipient areas L2a, the basorostral pallial nucleus, and the entopallium (corresponding to target areas for auditory, trigeminal and visual thalamic input, respectively) have been likened to layer IV of sensory cortices in mammals. In contrast, avian areas that receive input from these primary telencephalic areas (e.g. NCM and CMM, which receive auditory input from L2a) have been considered analogous to supragranular layers, and the arcopallium, which generates major descending telencephalic projections, has been argued to be analogous to infragranular layers of mammalian cortex. Our data in the zebra finch show that the primary thalamo-recipient telencephalic areas are largely devoid of labeling, whereas adjacent areas that receive input from these primary areas, in particular NCM and CMM, show sparse to moderate labeling. In addition, at least a portion of the arcopallium shows *Cck* labeling. Thus, in some general features, the cortical labeling pattern seems to be conserved in the avian pallium. This observation is consistent with the hypothesis that the various avian pallial fields derived from the dorsal ventricular ridge may

be homologous to different mammalian neocortical layers. One should note, however, that the labeling in the avian pallial fields is not as conspicuous as it appears in the mammalian cortical supra- and infragranular layers. In addition, the labeling in the arcopallium does not seem to correspond to the cell populations that originate descending projections, including RA and the adjacent cup region. Instead, the labeling is primarily in a dorsal region that is thought to receive input from the shell of lMAN (Bottjer et al., 2000; Bottjer and Johnson, 1997). Finally, we note that in mammals, parts of the claustrum, the endopiriform nucleus and several amygdalar nuclei, which may represent homologs of parts of the avian dorsal ventricular ridge also show significant *Cck* expression. Thus, although suggestive, the *Cck* expression data alone cannot be used as conclusive evidence for homologies between specific avian and mammalian pallial structures.

Another similarity in *Cck* expression between birds and mammals is the relatively high mRNA expression in the thalamus. In fact, the songbird thalamus presents some of the highest expression levels of *Cck* mRNA in the brain. In both vertebrate groups a large number of thalamic nuclei contain *Cck*-expressing cells. Interestingly, in the zebra finch, labeled cells are predominantly located within shell-like regions, with relatively few cells within the core portions of these nuclei (visual nucleus rotundus is a notable exception). It has been suggested based on cell morphology and connectivity that different cell populations occupy the core vs. shell portions of avian thalamic nuclei (Karten, 1967; Wild et al., 1993). Our present data are consistent with this interpretation and extend the notion that core and shell possess different neurochemical signatures.

Another prominent shared feature of *Cck* distribution is the expression of *Cck* in the medial and lateral portions of the dorsal raphe nuclei (Fig. 10A,B), and in dopaminergic cell group A11, the substantia nigra (SNr) and the ventral tegmental area (VTA). In mammals, the expression of *Cck* within these monoaminergic cell groups is thought to reflect an involvement of this neuropeptide in the regulation of functions like reward and satiety, which are known to be modulated by neurotransmitters like serotonin and catecholamines. We note that the percentage and distribution of dopaminergic neurons that co-localize with CCK in the SNr/VTA complex vary widely across mammals with the vast majority of dopaminergic cells in cats (Hokfelt et al., 1985) and monkeys being positive for CCK, but only few double-labeled cells being observed in hamsters (Miceli et al., 1987), hedgehogs (Antonopoulos et al., 1987), humans (Emson et al., 1982), and guinea pig (Ciofi and Tramu, 1990). In zebra finches, the relatively high abundance of *Cck* in the SNr/VTA may indicate that it plays a prominent role in dopamine reward pathways. This could include the pathways that are active during vocal learning, as has been suggested by gene expression and electrophysiology studies of the dopaminergic projection pathways to the song control system in the zebra finch (Nordeen et al., 2009; Gale and Perkel, 2010). Although the precise function of CCK in these pathways has not been tested, our data suggest a possible mechanism for influencing vocal learning through a direct release of CCK onto neurons in striatal area X of the song control system (further discussed below).

Intriguingly, the distribution of *Cck* in the striatum of rodents appears to be species-specific, with the striatum in rat, guinea pig, and hedgehog possessing clearly-labeled cells (Antonopoulos et al., 1987; Ciofi and Tramu, 1990; Marson et al., 1987; Takagi et al., 1984), and that of mouse being largely devoid of labeled cells. In the zebra finch, the striatum contains a sparse population of moderately labeled cells reminiscent of the distribution in rat. Thus, at least for a subset of mammals, the pattern of *Cck* expression in the striatum points to strong similarities in the neurochemical organization of basal ganglia in birds and mammals (Dutar et al., 1998; Farries and Perkel, 2002; Luo et al., 2001; Luo and Perkel, 1999; Person et al., 2008). The significance of species-dependent differences in striatal *Cck* are presently unknown

Despite the general similarities above, we also note significant differences that may reflect species differences in the overall organization of a CCK peptidergic system. Perhaps first and foremost, the vast majority of *Cck*-expressing cells in birds appear to be glutamatergic, as judged by their co-expression of the glutamatergic cell marker VGLUT2 in chicks and the lack of co-localization with the GABAergic cell marker *Gad65* in the zebra finch, whereas most CCK-expressing cells in mammals are thought to be GABAergic interneurons (Doetsch et al., 1993; Fallon et al., 1983; Kawaguchi and Kubota, 1998; Kubota and Kawaguchi, 1997; Seroogy et al., 1988; Somogyi et al., 1984). Of note, Maekawa et al. (2007) have argued that this apparent dichotomy may reflect a species difference in the frequency rather than phenotype of GABAergic versus glutamatergic cells in the pallium, as some studies have indicated that *Cck* is also expressed in pyramidal neurons of the rodent cortex that are thought to be largely glutamatergic (Burgunder and Young, 1990; Gallopin et al., 2006; Schiffmann et al., 1991).

We also note that the nucleus that has been identified as the avian thalamic reticular nucleus shows high *Cck* expression and that these *Cck*-expressing cells turned out to consist primarily of GABAergic neurons. This is in sharp contrast to mammals, where the reticular nucleus is negative for *Cck* mRNA, despite containing GABAergic cells (Esclapez et al., 1994; Esclapez et al., 1993; Feldblum et al., 1993). This discrepancy suggests that there may be species differences in the relative numbers of GABAergic versus non-GABAergic cells in birds and mammals, or possibly that the nucleus identified as the reticular nucleus in birds is not the true homolog the mammalian reticular nucleus. In the absence of further data, we currently favor the interpretation that this co-expression pattern represents an avian-(or perhaps songbird)-specific feature.

Our data also indicate that several discrete brain regions that show high expression of *Cck* in mammals, such as the medial portion of the habenula and cerebellar Purkinje cells, are virtually negative for *Cck* labeling in the zebra finch. The functional implications of such differences are currently unknown.

Is there a role for CCK in song auditory processing?

Song stimulation causes marked induction of gene expression in songbird NCM and CMM, both consisting of high-order auditory areas involved in the perceptual processing and memorization of song (Mello and Clayton, 1994; Mello et al., 2004). While this genomic response has been very useful for mapping the auditory representation of song, it also indicates that song triggers molecular events that may lead to the modification of the properties of song-responsive neurons, a process potentially underlying song perceptual memorization. Among song-induced genes, the expression of several rapidly induced immediate-early genes encoding transcription factors (*zenk* – a.k.a. *zif-268*, *egr-1*, *NGFI-A*, or *krox24*, *c-fos* and *c-jun*) or early effectors (*Arc*), as well as late effectors (synapsins 2 and 3) has been well characterized in NCM (Mello and Clayton, 1994; Mello et al., 1992; Velho and Mello, 2008; Velho et al., 2005). More recently, a plethora of candidate song-induced and -suppressed genes has been identified using microarray methodologies but different dissection strategies (Dong et al., 2009; Lovell and Mello, unpublished observations) or developmental ages (London et al., 2009). Among these candidates, *Cck* was found to undergo a marked induction 90 min after song stimulation. Our current data provide direct evidence that *Cck* mRNA is indeed induced in NCM by song stimulation, with a protracted time-course in comparison to early genes like *zenk* (Mello and Clayton, 1994; Velho et al., 2005). Even though we have not examined the CCK peptide or demonstrated a cellular co-localization of induced *zenk* and *Cck* mRNA, our data provide a likely link between song auditory processing and the regulation of the CCK peptide. Future studies will directly examine whether the *Cck* gene might be a downstream target of early regulators like ZENK.

Is NCM a primary site of action for locally produced CCK, or a source for song-regulated CCK that acts at other sites? While either view is possible, our double-labeling data indicate that the vast majority of *Cck*-expressing cells are non-GABAergic and most likely glutamatergic, which are more likely to include projection neurons. Thus at least some *Cck*-expressing cells in NCM might project to other brain areas. In fact, most *Cck*-expressing neurons in NCM in both song-stimulated and control birds are within rostral NCM (i.e. between L2a and the caudal domain defined by aromatase; Shen et al., 1994; Pinaud et al., 2006), which is thought to send projections into caudal NCM (Vates et al., 1996). As such, a local rostral-to-caudal circuit organization within NCM would allow CCK produced in rostral NCM to act at synapses in caudal NCM. It is also possible though that CCK produced in rostral NCM could affect areas outside NCM through longer-range projections. In support of this view, NCM is known to send projections to other auditory areas, including CMM and the lateral nidopallial shelf underneath song nucleus HVC, but the exact source of these projections within NCM is unknown. Alternatively, CCK could act locally in rostral NCM. An important next step will be to establish whether *Cck* is expressed in local interneurons or in cells that project to targets outside NCM.

Intriguingly, Ball et al., (1988) described abundant CCK-labeled fibers within a region immediately ventral and lateral to RA. The location of these fibers likely corresponds to the RA cup, a region within the arcopallium that receives projections from several nidopallial auditory areas, including subfields L1 and L3, and the shelf region ventral to HVC (Fig. 4E–F, 7D). Similar to the shelf, the RA cup responds to song with a robust *zenk* induction (Mello and Clayton, 1994). Since the shelf region contains a high density of *Cck*-labeled somata, it seems plausible that the labeled fibers in RA cup originate from the shelf and that the cup is a target of CCK modulation. Preliminary evidence indicates that the zebra finch ortholog of CCKBR (the major brain-expressed form of the CCK receptor) has a broad brain distribution, and is expressed at moderate levels in rostral NCM, besides several other pallial fields (Lovell and Mello, unpubl. obs). If confirmed, this observation would be consistent with data from the chick brain, where CCK and CCKBR show largely overlapping patterns (Maekawa et al., 2007). Altogether, in conjunction with previous studies (e.g. Ball et al., 1988), our data suggest that several levels of the auditory system, including NCM, the shelf and the RA cup, may be sources or targets for CCK modulation of auditory responses. Under this scenario, levels of CCK in the auditory pathway are likely to rise when a bird is exposed to conspecific song. Such an exposure would then be expected to exert its modulatory actions on the excitability of song-responsive circuits.

The precise physiological effect of CCK is not known. In mammals, there is growing evidence that CCK acts as an excitatory neurotransmitter or neuromodulator (Chung and Moore, 2007; Chung and Moore, 2009a; Chung and Moore, 2009b) that can enhance the intrinsic excitability of neurons by either decreasing a cell's permeability to potassium, or enhancing a non-selective cation current (Miller et al., 1997). For example, activation of CCKBR in the dentate gyrus has been shown to enhance GABA(A)-receptor-mediated synaptic transmission by inhibiting Ca^{2+}-activated K^{+} currents (Deng and Lei, 2006). Similar ionic mechanisms causing enhanced GABA(A) transmission have been proposed for the basolateral amygdala (Chhatwal et al., 2009; Chung and Moore, 2007) and hippocampus (Miller et al., 1997). In the cortex, pyramidal neurons have been shown to receive excitation from local clusters of GABAergic interneurons that express *Cck* (Chung and Moore, 2009a; Gallopin et al., 2006). Overall, such studies suggest that a major mode of action of CCK is to modulate local GABA-mediated inhibitory mechanisms. The predominance of GABAergic inhibition in NCM (Pinaud et al., 2008) suggests that local song-processing circuits in NCM could also be major CCK targets. Further studies on the exact cellular phenotype of cells expressing CCK and CCKBR are needed to further address this question in songbirds.

A possible link to cannabinoids and feeding behavior?

It is intriguing that the auditory response to novel song in NCM, as measured by ZENK expression, is very sensitive to feeding state, an effect that is thought to be mediated by endogenous cannabinoid signaling. Specifically, song-induced ZENK expression is decreased by limiting food intake, an effect that can be largely reversed by endocannabinoid antagonism (Soderstrom et al., 2004; Whitney et al., 2003). These findings have led to the notion that endocannabinoid signaling provides a link between song auditory processing and feeding state. Our current findings may bear direct relevance to this hypothesis. We show a clear upregulation of *Cck* expression in song-processing NCM neurons after song stimulation. In other systems, *Cck* expression has been shown to co-localize with CB1 receptors (Katona et al., 1999; Marsicano and Lutz, 1999), thus these two signaling systems can sometimes be tightly linked. In addition, there is increasing evidence that brain *Cck* may be involved in at least some aspects of the regulation of satiety (Moran and Kinzig, 2004; Valassi et al., 2008). These observations suggest the intriguing possibility that song-induced *Cck* regulation might also play a role in the regulation of satiety, or interact with the cannabinoid system and thus modulate the cannabinoid involvement in satiety and feeding behavior. Clearly more studies are required to better understand how these various systems interact, but the songbird model seems like an ideal organism to explore these questions further.

CCK modulation of the song system and singing behavior?

Our results both confirm and extend the findings of a previous study (Ball et al., 1988) that examined the immunohistochemical localization of the CCK peptide within the song system of the European starling and the song sparrow. Both studies detect a sparse population of labeled cells in mesencephalic ICo, particularly within song nucleus DM and auditory nucleus MLd, and a general lack of expression in telencephalic song nuclei HVC, lMAN, and RA. In the striatum, an area not investigated in the previous study, we also detect sparse labeling that includes song nucleus area X. However, the overall negative regulation of *Cck* in the song system suggests a general lack of involvement of *Cck* in vocal-motor control of song. Nevertheless, *Cck* could be involved in reward and/or motivational aspects of singing behavior. Consistent with mammals, we found that *Cck* is highly expressed in nuclei (e.g. VTA, SNr) that contain dopaminergic cell groups linked to reward and motivation (Girault and Greengard, 2004; Mehta and Riedel, 2006). These cell groups are thought to provide a major source of dopamine to the song system (Hara et al., 2007; Lewis et al., 1981). If these cells were to co-express *Cck,* as they are believed to do in mammals, they could provide the song system with CCK under specific behavioral contexts. For example, conditions that lead to the activation of catecholaminergic cell groups, such as hearing song or singing in a directed context (Sasaki et al., 2006), could potentially increase CCK release in the song system. The ensuing modulation of song-processing circuits by dopamine and/or CCK could then modulate the motivation to vocalize (sing and/or call) in response to the song presentation. Indeed, unilateral lesions to the SNr/VTA complex in male zebra finches reduce the rate of female-directed song, but not the rate, syllable structure, or stereotypy of undirected song, suggesting that this complex is more involved in the motivation to sing than in the vocal-motor control of singing (Hara et al., 2007). Further double-labeling analyses and electrophysiological recordings coupled to pharmacological manipulations will be required to clarify this issue.

In sum, the gut and brain peptide CCK is thought to play a role in the regulation of a broad range of neuronal functions, including anxiety-related and reward-related behaviors (Rotzinger et al., 2002; Rotzinger and Vaccarino, 2003), pain analgesia (Hebb et al., 2005), food intake (Dockray, 2009; Fogel et al., 2008; Konturek et al., 2004), and the acquisition and/or extinction of memories (Fride, 2005; Maekawa et al., 2007). The data we presented

here indicate that *Cck* expression is abundant within the songbird brain, is regulated by song presentation in a high-order auditory area involved in song perception and memorization, and is largely suppressed in the song system. These findings suggest a role for *Cck* in the regulation of different aspects of song behavior and pose intriguing questions for further research in the neurobiology of *Cck*.

Acknowledgments

Other acknowledgments We wish to thank Katy Horback for her extensive help with the histological preparations, development of the *in situ* hybridization protocol, and image capture and processing. We also acknowledge the support of NIH grant P30-NS06180, which provided imaging support for several of the figures presented in this manuscript.

Grant sponsor: NINDS Grant Numbers NS059755 and NS045264, and NIDCD Grant Number DC02853.

Literature Cited

Abercrombie M. Estimation of nuclear population from microtome sections. The Anatomical Record. 1946; 94(2):239–247. [PubMed: 21015608]

Amin N, Grace JA, Theunissen FE. Neural response to bird's own song and tutor song in the zebra finch field L and caudal mesopallium. J Comp Physiol A Neuroethol Sens Neural Behav Physiol. 2004; 190(6):469–489. [PubMed: 15064966]

Antonopoulos J, Papadopoulos GC, Karamanlidis AN, Parnavelas JG, Dinopoulos A, Michaloudi H. VIP- and CCK-like-immunoreactive neurons in the hedgehog (Erinaceus europaeus) and sheep (Ovis aries) brain. J Comp Neurol. 1987; 263(2):290–307. [PubMed: 3312309]

Bailey DJ, Wade J, Saldanha CJ. Hippocampal lesions impair spatial memory performance, but not song--a developmental study of independent memory systems in the zebra finch. Dev Neurobiol. 2009; 69(8):491–504. [PubMed: 19280648]

Ball GF, Faris PL, Hartman BK, Wingfield JC. Immunohistochemical localization of neuropeptides in the vocal control regions of two songbird species. Journal of Comparative Neurology. 1988; 268(2): 171–180. [PubMed: 2452178]

Bodanszky M, Martinez J, Priestley GP, Gardner JD, Mutt V. Cholecystokinin (pancreozymin). 4. Synthesis and properties of a biologically active analogue of the C-terminal heptapeptide with epsilon-hydroxynorleucine sulfate replacing tyrosine sulfate. J Med Chem. 1978; 21(10):1030–1035. [PubMed: 722712]

Bolhuis JJ, Eda-Fujiwara H. Bird brains and songs: neural mechanisms of birdsong perception and memory. Animal Biol. 2003; 53(2):129–145.

Bolhuis JJ, Hetebrij E, Den Boer-Visser AM, De Groot JH, Zijlstra GG. Localized immediate early gene expression related to the strength of song learning in socially reared zebra finches. Eur J Neurosci. 2001; 13(11):2165–2170. [PubMed: 11422458]

Bottjer SW, Arnold AP. The role of feedback from the vocal organ. I. Maintenance of stereotypical vocalizations by adult zebra finches. Journal of Neuroscience. 1984; 4(9):2387–2396. [PubMed: 6541246]

Bottjer SW, Brady JD, Cribbs B. Connections of a motor cortical region in zebra finches: relation to pathways for vocal learning. Journal of Comparative Neurology. 2000; 420(2):244–260. [PubMed: 10753310]

Bottjer SW, Halsema KA, Brown SA, Miesner EA. Axonal connections of a forebrain nucleus involved with vocal learning in zebra finches. J Comp Neurol. 1989; 279(2):312–326. [PubMed: 2464011]

Bottjer SW, Johnson F. Circuits, hormones, and learning: vocal behavior in songbirds. Journal of Neurobiology. 1997; 33(5):602–618. [PubMed: 9369462]

Brenowitz EA, Margoliash D, Nordeen KW. An introduction to birdsong and the avian song system. Journal of Neurobiology. 1997; 33(5):495–500. [PubMed: 9369455]

Burgunder JM, Young WS 3rd. The distribution of thalamic projection neurons containing cholecystokinin messenger RNA, using in situ hybridization histochemistry and retrograde labeling. Brain Res. 1988; 464(3):179–189. [PubMed: 3208109]

Burgunder JM, Young WS 3rd. Cortical neurons expressing the cholecystokinin gene in the rat: distribution in the adult brain, ontogeny, and some of their projections. J Comp Neurol. 1990; 300(1):26–46. [PubMed: 2229486]

Chew SJ, Mello C, Nottebohm F, Jarvis E, Vicario DS. Decrements in auditory responses to a repeated conspecific song are long-lasting and require two periods of protein synthesis in the songbird forebrain. Proc Natl Acad Sci U S A. 1995; 92(8):3406–3410. [PubMed: 7724575]

Chhatwal JP, Gutman AR, Maguschak KA, Bowser ME, Yang Y, Davis M, Ressler KJ. Functional interactions between endocannabinoid and CCK neurotransmitter systems may be critical for extinction learning. Neuropsychopharmacology. 2009; 34(2):509–521. [PubMed: 18580872]

Chung L, Moore SD. Cholecystokinin enhances GABAergic inhibitory transmission in basolateral amygdala. Neuropeptides. 2007; 41(6):453–463. [PubMed: 17904218]

Chung L, Moore SD. Cholecystokinin excites interneurons in rat basolateral amygdala. J Neurophysiol. 2009a; 102(1):272–284. [PubMed: 19386755]

Chung L, Moore SD. Neuropeptides modulate compound postsynaptic potentials in basolateral amygdala. Neuroscience. 2009b; 164(4):1389–1397. [PubMed: 19786076]

Ciofi P, Tramu G. Distribution of cholecystokinin-like-immunoreactive neurons in the guinea pig forebrain. J Comp Neurol. 1990; 300(1):82–112. [PubMed: 2229489]

Deng PY, Lei S. Bidirectional modulation of GABAergic transmission by cholecystokinin in hippocampal dentate gyrus granule cells of juvenile rats. J Physiol. 2006; 572(Pt 2):425–442. [PubMed: 16455686]

Dockray GJ. Cholecystokinin and gut-brain signalling. Regul Pept. 2009; 155(1–3):6–10. [PubMed: 19345244]

Doetsch GS, Norelle A, Mark EK, Standage GP, Lu SM, Lin RC. Immunoreactivity for GAD and three peptides in somatosensory cortex and thalamus of the raccoon. Brain Res Bull. 1993; 31(5): 553–563. [PubMed: 8098654]

Dong S, Replogle KL, Hasadsri L, Imai BS, Yau PM, Rodriguez-Zas S, Southey BR, Sweedler JV, Clayton DF. Discrete molecular states in the brain accompany changing responses to a vocal signal. Proc Natl Acad Sci U S A. 2009; 106(27):11364–11369. [PubMed: 19541599]

Dutar P, Vu HM, Perkel DJ. Multiple cell types distinguished by physiological, pharmacological, and anatomic properties in nucleus HVc of the adult zebra finch. J Neurophysiol. 1998; 80(4):1828–1838. [PubMed: 9772242]

Emson PC, Rehfeld JF, Rossor MN. Distribution of cholecystokinin-like peptides in the human-brain. J Neurochem. 1982; 38(4):1177–1179. [PubMed: 7062038]

Erichsen JT, Bingman VP, Krebs JR. The distribution of neuropeptides in the dorsomedial telencephalon of the pigeon (Columba livia): a basis for regional subdivisions. J Comp Neurol. 1991; 314(3):478–492. [PubMed: 1726107]

Esclapez M, Tillakaratne NJ, Kaufman DL, Tobin AJ, Houser CR. Comparative localization of two forms of glutamic acid decarboxylase and their mRNAs in rat brain supports the concept of functional differences between the forms. J Neurosci. 1994; 14(3 Pt 2):1834–1855. [PubMed: 8126575]

Esclapez M, Tillakaratne NJ, Tobin AJ, Houser CR. Comparative localization of mRNAs encoding two forms of glutamic acid decarboxylase with nonradioactive in situ hybridization methods. J Comp Neurol. 1993; 331(3):339–362. [PubMed: 8514913]

Fallon JH, Seroogy KB. Visual and auditory pathways contain cholecystokinin: evidence from immunofluorescence and retrograde tracing. Neurosci Lett. 1984; 45(1):81–87. [PubMed: 6374513]

Fallon JH, Wang C, Kim Y, Canepa N, Loughlin S, Seroogy K. Dopamine- and cholecystokinin-containing neurons of the crossed mesostriatal projection. Neurosci Lett. 1983; 40(3):233–238. [PubMed: 6316210]

Farries MA, Perkel DJ. A telencephalic nucleus essential for song learning contains neurons with physiological characteristics of both striatum and globus pallidus. Journal of Neuroscience. 2002; 22(9):3776–3787. [PubMed: 11978853]

Feldblum S, Erlander MG, Tobin AJ. Different distributions of GAD65 and GAD67 mRNAs suggest that the two glutamate decarboxylases play distinctive functional roles. J Neurosci Res. 1993; 34(6):689–706. [PubMed: 8315667]

Fogel WA, Stasiak A, Lewinski A, Maksymowicz M, Jochem J. Satiety signalling histaminergic system and brain-gut peptides in regulation of food intake in rats with portocaval anastomosis. J Physiol Pharmacol. 2008; 59 Suppl 2:135–144. [PubMed: 18812634]

Fox CA, Jeyapalan M, Ross LR, Jacobson CD. Ontogeny of cholecystokinin-like immunoreactivity in the Brazilian opossum brain. Brain Res Dev Brain Res. 1991; 64(1–2):1–18.

Fride E. Endocannabinoids in the central nervous system: from neuronal networks to behavior. Curr Drug Targets CNS Neurol Disord. 2005; 4(6):633–642. [PubMed: 16375681]

Gagliardo A, Ioale P, Bingman VP. Homing in pigeons: the role of the hippocampal formation in the representation of landmarks used for navigation. J Neurosci. 1999; 19(1):311–315. [PubMed: 9870960]

Gale SD, Perkel DJ. A basal ganglia pathway drives selective auditory responses in songbird dopaminergic neurons via disinhibition. J Neurosci. 2010; 30(3):1027–1037. [PubMed: 20089911]

Gallopin T, Geoffroy H, Rossier J, Lambolez B. Cortical sources of CRF, NKB, and CCK and their effects on pyramidal cells in the neocortex. Cereb Cortex. 2006; 16(10):1440–1452. [PubMed: 16339088]

Girault JA, Greengard P. The neurobiology of dopamine signaling. Arch Neurol. 2004; 61(5):641–644. [PubMed: 15148138]

Gobes SM, Bolhuis JJ. Birdsong memory: a neural dissociation between song recognition and production. Curr Biol. 2007; 17(9):789–793. [PubMed: 17433683]

Grace JA, Amin N, Singh NC, Theunissen FE. Selectivity for conspecific song in the zebra finch auditory forebrain. J Neurophysiol. 2003; 89(1):472–487. [PubMed: 12522195]

Hara E, Kubikova L, Hessler NA, Jarvis ED. Role of the midbrain dopaminergic system in modulation of vocal brain activation by social context. Eur J Neurosci. 2007; 25(11):3406–3416. [PubMed: 17553009]

Hauber ME, Cassey P, Woolley SM, Theunissen FE. Neurophysiological response selectivity for conspecific songs over synthetic sounds in the auditory forebrain of non-singing female songbirds. J Comp Physiol A Neuroethol Sens Neural Behav Physiol. 2007; 193(7):765–774. [PubMed: 17503053]

Hebb AL, Poulin JF, Roach SP, Zacharko RM, Drolet G. Cholecystokinin and endogenous opioid peptides: interactive influence on pain, cognition, and emotion. Prog Neuropsychopharmacol Biol Psychiatry. 2005; 29(8):1225–1238. [PubMed: 16242828]

Hokfelt T, Skirboll L, Everitt B, Meister B, Brownstein M, Jacobs T, Faden A, Kuga S, Goldstein M, Markstein R, et al. Distribution of cholecystokinin-like immunoreactivity in the nervous system. Co-existence with classical neurotransmitters and other neuropeptides. Ann N Y Acad Sci. 1985; 448:255–274. [PubMed: 2411182]

Huntley GW, Jones EG. The emergence of architectonic field structure and areal borders in developing monkey sensorimotor cortex. Neuroscience. 1991; 44(2):287–310. [PubMed: 1719447]

Ingram SM, Krause RG 2nd, Baldino F Jr, Skeen LC, Lewis ME. Neuronal localization of cholecystokinin mRNA in the rat brain by using in situ hybridization histochemistry. J Comp Neurol. 1989; 287(2):260–272. [PubMed: 2794128]

Jarvis ED, Gunturkun O, Bruce L, Csillag A, Karten H, Kuenzel W, Medina L, Paxinos G, Perkel DJ, Shimizu T, Striedter G, Wild JM, Ball GF, Dugas-Ford J, Durand SE, Hough GE, Husband S, Kubikova L, Lee DW, Mello CV, Powers A, Siang C, Smulders TV, Wada K, White SA, Yamamoto K, Yu J, Reiner A, Butler AB. Avian brains and a new understanding of vertebrate brain evolution. Nat Rev Neurosci. 2005; 6(2):151–159. [PubMed: 15685220]

Jinno S, Kosaka T. Heterogeneous expression of the cholecystokinin-like immunoreactivity in the mouse hippocampus, with special reference to the dorsoventral difference. Neuroscience. 2003; 122(4):869–884. [PubMed: 14643757]

Karten HJ. The organization of the ascending auditory pathway in the pigeon (*Columba livia*). I. Diencephalic projections of the inferior colliculus (nucleus mesencephali lateralis, pars dorsalis). Brain Research. 1967; 6(3):409–427. [PubMed: 6076249]

Karten, HJ.; Hodos, WA. A Stereotaxic Atlas of the Brain of the Pigeon (Columba livia). Baltimore, MD: Johns Hopkins University Press; 1966.

Katona I, Sperlagh B, Sik A, Kafalvi A, Vizi ES, Mackie K, Freund TF. Presynaptically located CB1 cannabinoid receptors regulate GABA release from axon terminals of specific hippocampal interneurons. J Neurosci. 1999; 19(11):4544–4558. [PubMed: 10341254]

Kawaguchi Y, Kondo S. Parvalbumin, somatostatin and cholecystokinin as chemical markers for specific GABAergic interneuron types in the rat frontal cortex. J Neurocytol. 2002; 31(3–5):277–287. [PubMed: 12815247]

Kawaguchi Y, Kubota Y. Neurochemical features and synaptic connections of large physiologically-identified GABAergic cells in the rat frontal cortex. Neuroscience. 1998; 85(3):677–701. [PubMed: 9639265]

Kelley DB, Nottebohm F. Projections of a telencephalic auditory nucleus-field L-in the canary. Journal of Comparative Neurology. 1979; 183(3):455–469. [PubMed: 759444]

Klausberger T, Marton LF, O'Neill J, Huck JH, Dalezios Y, Fuentealba P, Suen WY, Papp E, Kaneko T, Watanabe M, Csicsvari J, Somogyi P. Complementary roles of cholecystokinin- and parvalbumin-expressing GABAergic neurons in hippocampal network oscillations. J Neurosci. 2005; 25(42):9782–9793. [PubMed: 16237182]

Konturek SJ, Konturek JW, Pawlik T, Brzozowski T. Brain-gut axis and its role in the control of food intake. J Physiol Pharmacol. 2004; 55(1 Pt 2):137–154. [PubMed: 15082874]

Krebs JR, Erichsen JT, Bingman VP. The distribution of neurotransmitters and neurotransmitter-related enzymes in the dorsomedial telencephalon of the pigeon (Columba livia). J Comp Neurol. 1991; 314(3):467–477. [PubMed: 1687688]

Kubota Y, Kawaguchi Y. Two distinct subgroups of cholecystokinin-immunoreactive cortical interneurons. Brain Res. 1997; 752(1–2):175–183. [PubMed: 9106454]

Kuenzel, WJ.; Masson, M. A Stereotaxic Atlas of the Brain of the chick (Gallus domesticus). Baltimore, MD: Johns Hopkins University Press; 1988.

Lein ES, Hawrylycz MJ, Ao N, Ayres M, Bensinger A, Bernard A, Boe AF, Boguski MS, Brockway KS, Byrnes EJ, Chen L, Chen TM, Chin MC, Chong J, Crook BE, Czaplinska A, Dang CN, Datta S, Dee NR, Desaki AL, Desta T, Diep E, Dolbeare TA, Donelan MJ, Dong HW, Dougherty JG, Duncan BJ, Ebbert AJ, Eichele G, Estin LK, Faber C, Facer BA, Fields R, Fischer SR, Fliss TP, Frensley C, Gates SN, Glattfelder KJ, Halverson KR, Hart MR, Hohmann JG, Howell MP, Jeung DP, Johnson RA, Karr PT, Kawal R, Kidney JM, Knapik RH, Kuan CL, Lake JH, Laramee AR, Larsen KD, Lau C, Lemon TA, Liang AJ, Liu Y, Luong LT, Michaels J, Morgan JJ, Morgan RJ, Mortrud MT, Mosqueda NF, Ng LL, Ng R, Orta GJ, Overly CC, Pak TH, Parry SE, Pathak SD, Pearson OC, Puchalski RB, Riley ZL, Rockett HR, Rowland SA, Royall JJ, Ruiz MJ, Sarno NR, Schaffnit K, Shapovalova NV, Sivisay T, Slaughterbeck CR, Smith SC, Smith KA, Smith BI, Sodt AJ, Stewart NN, Stumpf KR, Sunkin SM, Sutram M, Tam A, Teemer CD, Thaller C, Thompson CL, Varnam LR, Visel A, Whitlock RM, Wohnoutka PE, Wolkey CK, Wong VY, Wood M, Yaylaoglu MB, Young RC, Youngstrom BL, Yuan XF, Zhang B, Zwingman TA, Jones AR. Genome-wide atlas of gene expression in the adult mouse brain. Nature. 2007; 445(7124):168–176. [PubMed: 17151600]

Lewis JW, Ryan SM, Arnold AP, Butcher LL. Evidence for a catecholaminergic projection to area X in the zebra finch. Journal of Comparative Neurology. 1981; 196(2):347–354. [PubMed: 7217361]

London SE, Clayton DF. Functional identification of sensory mechanisms required for developmental song learning. Nat Neurosci. 2008; 11(5):579–586. [PubMed: 18391944]

London SE, Dong S, Replogle K, Clayton DF. Developmental shifts in gene expression in the auditory forebrain during the sensitive period for song learning. Dev Neurobiol. 2009; 69(7):437–450. [PubMed: 19360720]

Lovell PV, Clayton DF, Replogle KL, Mello CV. Birdsong "transcriptomics": neurochemical specializations of the oscine song system. PLoS ONE. 2008; 3(10):e3440. [PubMed: 18941504]

Luo M, Ding L, Perkel DJ. An avian basal ganglia pathway essential for vocal learning forms a closed topographic loop. J Neurosci. 2001; 21(17):6836–6845. [PubMed: 11517271]

Luo M, Perkel DJ. Long-range GABAergic projection in a circuit essential for vocal learning. J Comp Neurol. 1999; 403(1):68–84. [PubMed: 10075444]

Maekawa F, Nakamori T, Uchimura M, Fujiwara K, Yada T, Tsukahara S, Kanamatsu T, Tanaka K, Ohki-Hamazaki H. Activation of cholecystokinin neurons in the dorsal pallium of the telencephalon is indispensable for the acquisition of chick imprinting behavior. J Neurochem. 2007; 102(5):1645–1657. [PubMed: 17697050]

Marsicano G, Lutz B. Expression of the cannabinoid receptor CB1 in distinct neuronal subpopulations in the adult mouse forebrain. Eur J Neurosci. 1999; 11(12):4213–4225. [PubMed: 10594647]

Marson L, Lauterio TJ, Della-Fera MA, Baile CA. Immunohistochemical distribution of cholecystokinin, dynorphin A and Met-enkephalin neurons in sheep hypothalamus. Neurosci Lett. 1987; 81(1–2):35–40. [PubMed: 2892157]

Mehta MA, Riedel WJ. Dopaminergic enhancement of cognitive function. Curr Pharm Des. 2006; 12(20):2487–2500. [PubMed: 16842172]

Mello, CV. Analysis of immediate early gene expression in the songbird brain following song presentation. New York: The Rockefeller University; 1993.

Mello CV. Auditory experience, gene regulation and auditory memories in songbirds. Journal of the Brazilian Association for the Advancement of Science. 1998; 50:189–196.

Mello CV, Clayton DF. Song-induced ZENK gene expression in auditory pathways of songbird brain and its relation to the song control system. J Neurosci. 1994; 14(11 Pt 1):6652–6666. [PubMed: 7965067]

Mello CV, Velho TA, Pinaud R. Song-induced gene expression: a window on song auditory processing and perception. Ann N Y Acad Sci. 2004; 1016:263–281. [PubMed: 15313780]

Mello CV, Vicario DS, Clayton DF. Song presentation induces gene expression in the songbird forebrain. Proc Natl Acad Sci U S A. 1992; 89(15):6818–6822. [PubMed: 1495970]

Meziane H, Devigne C, Tramu G, Soumireu-Mourat B. Distribution of cholecystokinin immunoreactivity in the BALB/c mouse forebrain: an immunocytochemical study. J Chem Neuroanat. 1997; 12(3):191–209. [PubMed: 9141651]

Miceli MO, van der Kooy D, Post CA, Della-Fera MA, Baile CA. Differential distributions of cholecystokinin in hamster and rat forebrain. Brain Res. 1987; 402(2):318–330. [PubMed: 3828799]

Micevych P, Akesson T, Elde R. Distribution of cholecystokinin-immunoreactive cell bodies in the male and female rat: II. Bed nucleus of the stria terminalis and amygdala. J Comp Neurol. 1988; 269(3):381–391. [PubMed: 3372720]

Miller KK, Hoffer A, Svoboda KR, Lupica CR. Cholecystokinin increases GABA release by inhibiting a resting K+ conductance in hippocampal interneurons. J Neurosci. 1997; 17(13):4994–5003. [PubMed: 9185537]

Moran TH, Kinzig KP. Gastrointestinal satiety signals II. Cholecystokinin. Am J Physiol Gastrointest Liver Physiol. 2004; 286(2):G183–G188. [PubMed: 14715515]

Morino P, Herrera-Marschitz M, Castel MN, Ungerstedt U, Varro A, Dockray G, Hokfelt T. Cholecystokinin in cortico-striatal neurons in the rat: immunohistochemical studies at the light and electron microscopical level. Eur J Neurosci. 1994; 6(5):681–692. [PubMed: 7915604]

Ng L, Bernard A, Lau C, Overly CC, Dong HW, Kuan C, Pathak S, Sunkin SM, Dang C, Bohland JW, Bokil H, Mitra PP, Puelles L, Hohmann J, Anderson DJ, Lein ES, Jones AR, Hawrylycz M. An anatomic gene expression atlas of the adult mouse brain. Nat Neurosci. 2009; 12(3):356–362. [PubMed: 19219037]

Nixdorf-Bergweiler, BEBH-J. A stereotaxic atlas of the brain of the zebra finch, Taeniopygia guttata, with special special emphasis on telencephalic visual and song system nuclei in transverse and sagittal sections. Bethesda: National Library of Medicine, National Center for Biotechnology Information;

Nordeen EJ, Holtzman DA, Nordeen KW. Increased Fos expression among midbrain dopaminergic cell groups during birdsong tutoring. Eur J Neurosci. 2009; 30(4):662–670. [PubMed: 19686474]

Ogawa R, Itoh K, Kaneko T, Mizuno N. Co-existence of vasoactive intestinal polypeptide (VIP)- and cholecystokinin (CCK)-like immunoreactivities in thalamocortical neuron in the ventrolateral nucleus of the rat. Brain Res. 1989; 490(1):152–156. [PubMed: 2758323]

Person AL, Gale SD, Farries MA, Perkel DJ. Organization of the songbird basal ganglia, including area X. J Comp Neurol. 2008; 508(5):840–866. [PubMed: 18398825]

Pinaud R, Fortes AF, Lovell P, Mello CV. Calbindin-positive neurons reveal a sexual dimorphism within the songbird analogue of the mammalian auditory cortex. J Neurobiol. 2006; 66(2):182–195. [PubMed: 16288476]

Pinaud R, Terleph TA, Tremere LA, Phan ML, Dagostin AA, Leao RM, Mello CV, Vicario DS. Inhibitory network interactions shape the auditory processing of natural communication signals in the songbird auditory forebrain. J Neurophysiol. 2008; 100(1):441–455. [PubMed: 18480371]

Pinaud R, Velho TA, Jeong JK, Tremere LA, Leao RM, von Gersdorff H, Mello CV. GABAergic neurons participate in the brain's response to birdsong auditory stimulation. Eur J Neurosci. 2004; 20(5):1318–1330. [PubMed: 15341603]

Puelles, L.; Paxinos, G.; Watson, C.; Martinez, S.; Martinez-de-la-Torre, M. The Chick Brain in Stereotaxic Coordinates: An Atlas Based on Neuromeres. Elsevier Science & Technology Books; 2007.

Reiner A, Perkel DJ, Bruce LL, Butler AB, Csillag A, Kuenzel W, Medina L, Paxinos G, Shimizu T, Striedter G, Wild M, Ball GF, Durand S, Gunturkun O, Lee DW, Mello CV, Powers A, White SA, Hough G, Kubikova L, Smulders TV, Wada K, Dugas-Ford J, Husband S, Yamamoto K, Yu J, Siang C, Jarvis ED. Revised nomenclature for avian telencephalon and some related brainstem nuclei. J Comp Neurol. 2004; 473(3):377–414. [PubMed: 15116397]

Ribeiro S, Cecchi GA, Magnasco MO, Mello CV. Toward a song code: evidence for a syllabic representation in the canary brain. Neuron. 1998; 21(2):359–371. [PubMed: 9728917]

Rotzinger S, Bush DE, Vaccarino FJ. Cholecystokinin modulation of mesolimbic dopamine function: regulation of motivated behaviour. Pharmacol Toxicol. 2002; 91(6):404–413. [PubMed: 12688386]

Rotzinger S, Vaccarino FJ. Cholecystokinin receptor subtypes: role in the modulation of anxiety-related and reward-related behaviours in animal models. J Psychiatry Neurosci. 2003; 28(3):171–181. [PubMed: 12790157]

Sasaki A, Sotnikova TD, Gainetdinov RR, Jarvis ED. Social context-dependent singing-regulated dopamine. J Neurosci. 2006; 26(35):9010–9014. [PubMed: 16943558]

Savasta M, Ruberte E, Palacios JM, Mengod G. The colocalization of cholecystokinin and tyrosine hydroxylase mRNAs in mesencephalic dopaminergic neurons in the rat brain examined by in situ hybridization. Neuroscience. 1989; 29(2):363–369. [PubMed: 2566954]

Schiffmann SN, Teugels E, Halleux P, Menu R, Vanderhaeghen JJ. Cholecystokinin mRNA detection in rat spinal cord motoneurons but not in dorsal root ganglia neurons. Neurosci Lett. 1991; 123(1):123–126. [PubMed: 2062448]

Schiffmann SN, Vanderhaeghen JJ. Distribution of cells containing mRNA encoding cholecystokinin in the rat central nervous system. J Comp Neurol. 1991; 304(2):219–233. [PubMed: 2016418]

Seroogy K, Ceccatelli S, Schalling M, Hokfelt T, Frey P, Walsh J, Dockray G, Brown J, Buchan A, Goldstein M. A subpopulation of dopaminergic neurons in rat ventral mesencephalon contains both neurotensin and cholecystokinin. Brain Res. 1988; 455(1):88–98. [PubMed: 3046712]

Shen P, Campagnoni CW, Kampf K, Schlinger BA, Arnold AP, Campagnoni AT. Isolation and characterization of a zebra finch aromatase cDNA: in situ hybridization reveals high aromatase expression in brain. Brain Res Mol Brain Res. 1994; 24(1–4):227–237. [PubMed: 7968362]

Soderstrom K, Tian Q, Valenti M, Di Marzo V. Endocannabinoids link feeding state and auditory perception-related gene expression. J Neurosci. 2004; 24(44):10013–10021. [PubMed: 15525787]

Sohrabji F, Nordeen KW, Nordeen EJ. Projections of androgen-accumulating neurons in a nucleus controlling avian song. Brain Res. 1989; 488(1–2):253–259. [PubMed: 2743120]

Somogyi P, Hodgson AJ, Smith AD, Nunzi MG, Gorio A, Wu JY. Different populations of GABAergic neurons in the visual cortex and hippocampus of cat contain somatostatin- or

cholecystokinin-immunoreactive material. J Neurosci. 1984; 4(10):2590–2603. [PubMed: 6149275]

Stokes TM, Leonard CM, Nottebohm F. The telencephalon, diencephalon, and mesencephalon of the canary, Serinus canaria, in stereotaxic coordinates. J Comp Neurol. 1974; 156(3):337–374. [PubMed: 4609173]

Stripling R, Volman SF, Clayton DF. Response modulation in the zebra finch neostriatum: relationship to nuclear gene regulation. J Neurosci. 1997; 17(10):3883–3893. [PubMed: 9133406]

Szekely AD, Krebs JR. Efferent connectivity of the hippocampal formation of the zebra finch (Taenopygia guttata): an anterograde pathway tracing study using Phaseolus vulgaris leucoagglutinin. J Comp Neurol. 1996; 368(2):198–214. [PubMed: 8725302]

Takagi H, Kubota Y, Mori S, Tateishi K, Hamaoka T, Tohyama M. Fine structural studies of cholecystokinin-8-like immunoreactive neurons and axon terminals in the nucleus of tractus solitarius of the rat. J Comp Neurol. 1984; 227(3):369–379. [PubMed: 6090510]

Terleph TA, Mello CV, Vicario DS. Auditory topography and temporal response dynamics of canary caudal telencephalon. J Neurobiol. 2006; 66(3):281–292. [PubMed: 16329130]

Terleph TA, Mello CV, Vicario DS. Species differences in auditory processing dynamics in songbird auditory telencephalon. Dev Neurobiol. 2007; 67(11):1498–1510. [PubMed: 17525994]

Valassi E, Scacchi M, Cavagnini F. Neuroendocrine control of food intake. Nutr Metab Cardiovasc Dis. 2008; 18(2):158–168. [PubMed: 18061414]

Vargas JP, Petruso EJ, Bingman VP. Hippocampal formation is required for geometric navigation in pigeons. Eur J Neurosci. 2004; 20(7):1937–1944. [PubMed: 15380016]

Vates GE, Broome BM, Mello CV, Nottebohm F. Auditory pathways of caudal telencephalon and their relation to the song system of adult male zebra finches. J Comp Neurol. 1996; 366(4):613–642. [PubMed: 8833113]

Vates GE, Vicario DS, Nottebohm F. Reafferent thalamo- "cortical" loops in the song system of oscine songbirds. J Comp Neurol. 1997; 380(2):275–290. [PubMed: 9100137]

Velho TA, Mello CV. Synapsins are late activity-induced genes regulated by birdsong. J Neurosci. 2008; 28(46):11871–11882. [PubMed: 19005052]

Velho TA, Pinaud R, Rodrigues PV, Mello CV. Co-induction of activity-dependent genes in songbirds. Eur J Neurosci. 2005; 22(7):1667–1678. [PubMed: 16197507]

Voigt MM, Uhl GR. Preprocholecystokinin mRNA in rat brain: regional expression includes thalamus. Brain Res. 1988; 464(3):247–253. [PubMed: 3208111]

Watanabe S. Effects of hippocampal lesions on repeated acquisition of spatial discrimination in pigeons. Behav Brain Res. 2001; 120(1):59–66. [PubMed: 11173085]

Whitney O, Soderstrom K, Johnson F. CB1 cannabinoid receptor activation inhibits a neural correlate of song recognition in an auditory/perceptual region of the zebra finch telencephalon. J Neurobiol. 2003; 56(3):266–274. [PubMed: 12884265]

Wild JM, Karten HJ, Frost BJ. Connections of the auditory forebrain in the pigeon (Columba livia). J Comp Neurol. 1993; 337(1):32–62. [PubMed: 8276991]

Woolley SC, Doupe AJ. Social context-induced song variation affects female behavior and gene expression. PLoS Biol. 2008; 6(3):e62. [PubMed: 18351801]

Zeigler, HP.; Marler, P., editors. Ann. NY Acad. Sci. 2004. Behavioral Neurobiology of Birdsong.

Zeigler, HP.; Marler, P., editors. Neuroscience of Birdsong. Cambridge, UK: Cambridge University Press; 2008.

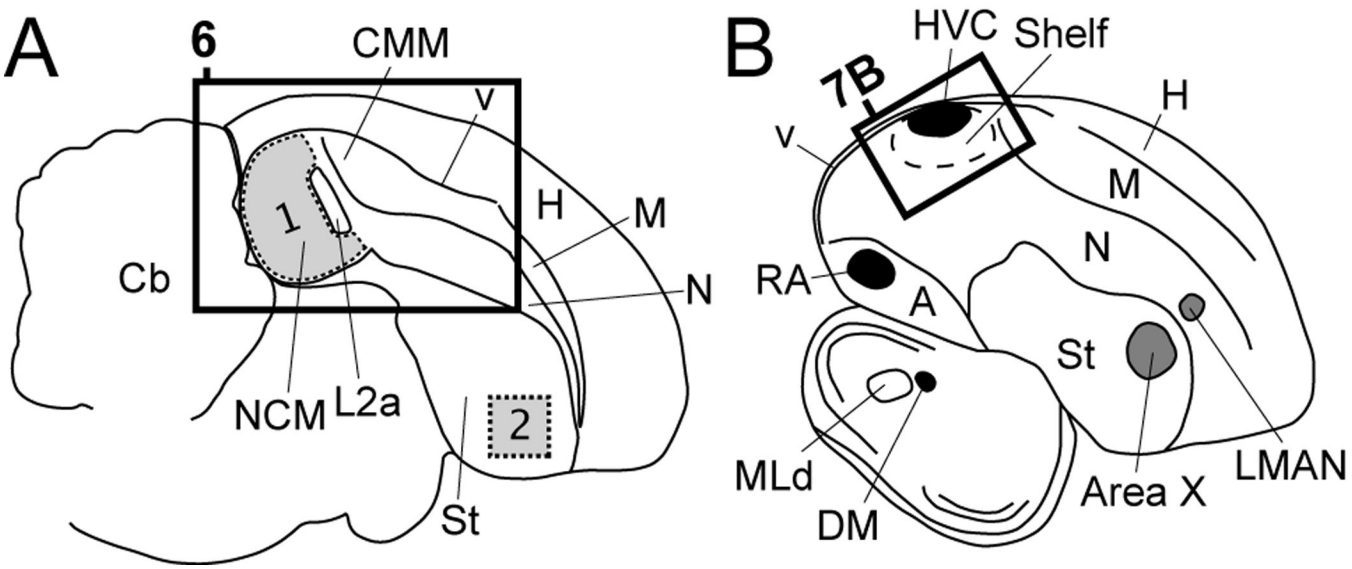

Figure 1.

Camera lucida drawings of parasagittal brain sections from an adult male zebra finch at ~0.6 mm (**A**), and ~2.4 mm (**B**) from the midline. Rectangles in A and B indicate the positions of the photomicrographs in Figures 6 and 7D, respectively. **A**: Region over which optical densitometry for *Cck* mRNA and *Cck* cell counts were performed (presented in Figure 12) are depicted in grey for auditory NCM (region 1) and a non-auditory region of the medial striatum (region 2). **B**: The major nuclei of the song system that underlie vocal learning and singing behavior in songbirds are depicted in grey and black, respectively. The song system is composed of a direct motor pathway consisting of projections from HVC to RA, from RA to DM and motor neurons of the tracheosyringeal nucleus (nXIIts) of the medulla, or to brainstem nuclei involved in respiratory control (Bottjer and Arnold, 1984; Sohrabji et al., 1989; Vates et al., 1997; Wild et al., 1997), and an indirect pathway that includes a projection loop from Area X in the striatum to thalamic DLM (not depicted in Fig. 1B), from DLM to LMAN, and from LMAN back to area X (Bottjer et al., 1989; Luo et al., 2001; Vates et al., 1997). For abbreviations see Table 1.

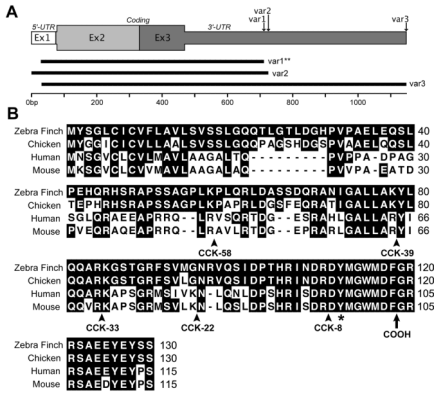

Figure 2.

The zebra finch *Cck* gene. **A**: The gene encoding *Cck* is represented by three exons (Ex1–3) that span a ~7 kb region of chromosome 2. At least three transcript variants of *Cck* (var1–3; 100% identical within their predicted peptide coding regions) are found in the zebra finch brain based on EST evidence; these differ according to the length of their 3'-untranslated region prior to a predicted poly-adenylation tag. A single clone representing *Cck* var1 (**; CK302967) was used to derive probes for all of the *in situ* hybridization data presented here; similar results were obtained using a clone representing the longer *Cck* var3 (CK314171). **B**: Alignment of the predicted amino acid sequence of zebra finch CCK protein with orthologs from chicken, human and mouse. Numbers on the right indicate the relative position of amino acid residues in each sequence; conserved amino acid residues for any position are in shaded in black. Arrows indicate the predicted cleavage sites for various CCK peptide products. A conserved tyrosine residue at position 122 of the zebra finch sequence, which is typically sulfanated, is indicated by an asterisk. The location of the carboxy-terminus of the peptide after final cleavage is indicated with an arrow.

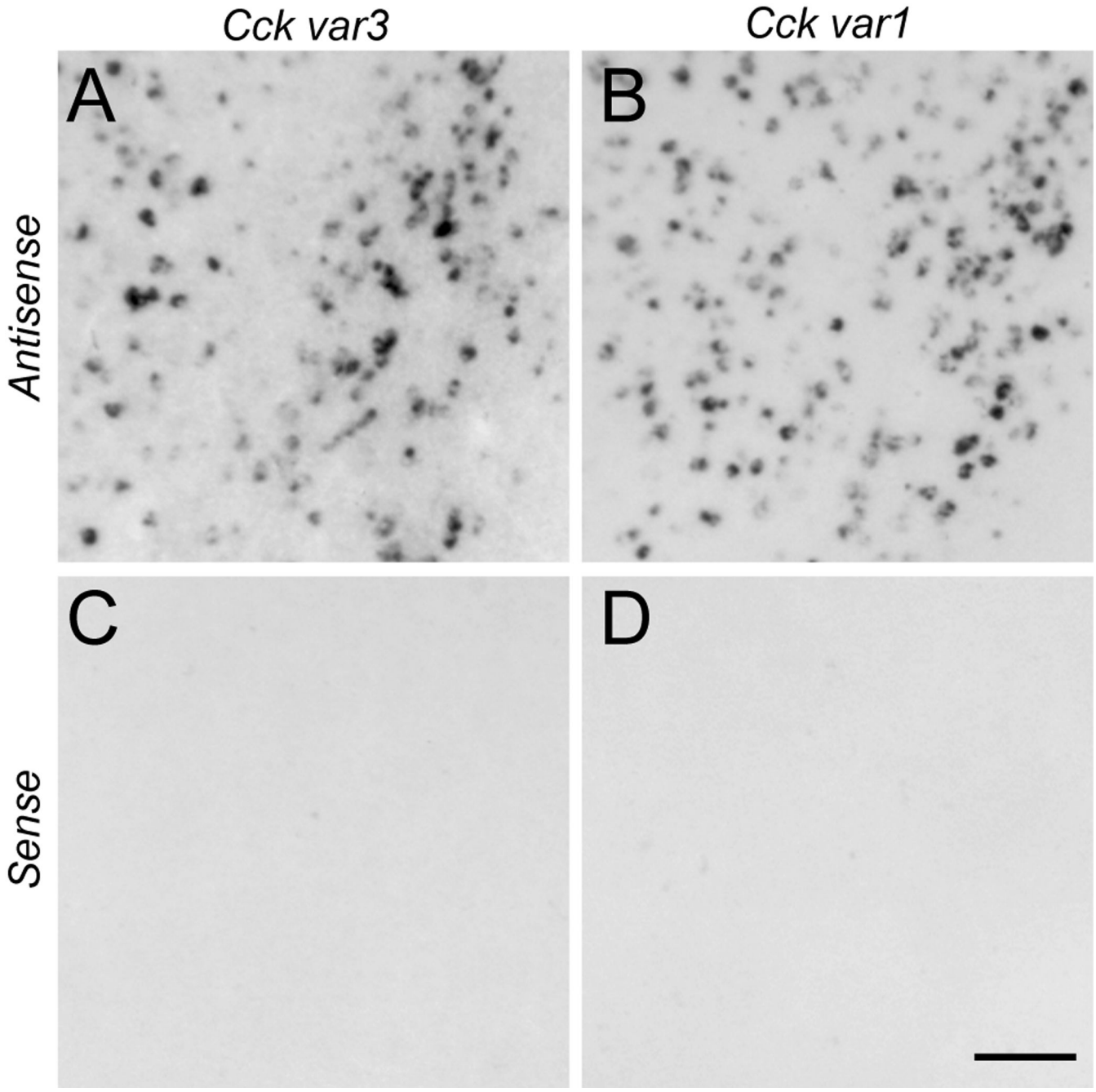

Figure 3.
Comparison of *Cck* mRNA expression in the rostromedial nidopallium as revealed by *in situ* hybridization of antisense (**A**, **B**) and sense (**C**, **D**) strand riboprobes targeting *Cck* variants 3 (**A**, **C**) and 1 (**B**, **D**) in serial parasagittal brain sections from an adult male zebra finch (~0.6 mm from the midline). Scale bar: 100μm.

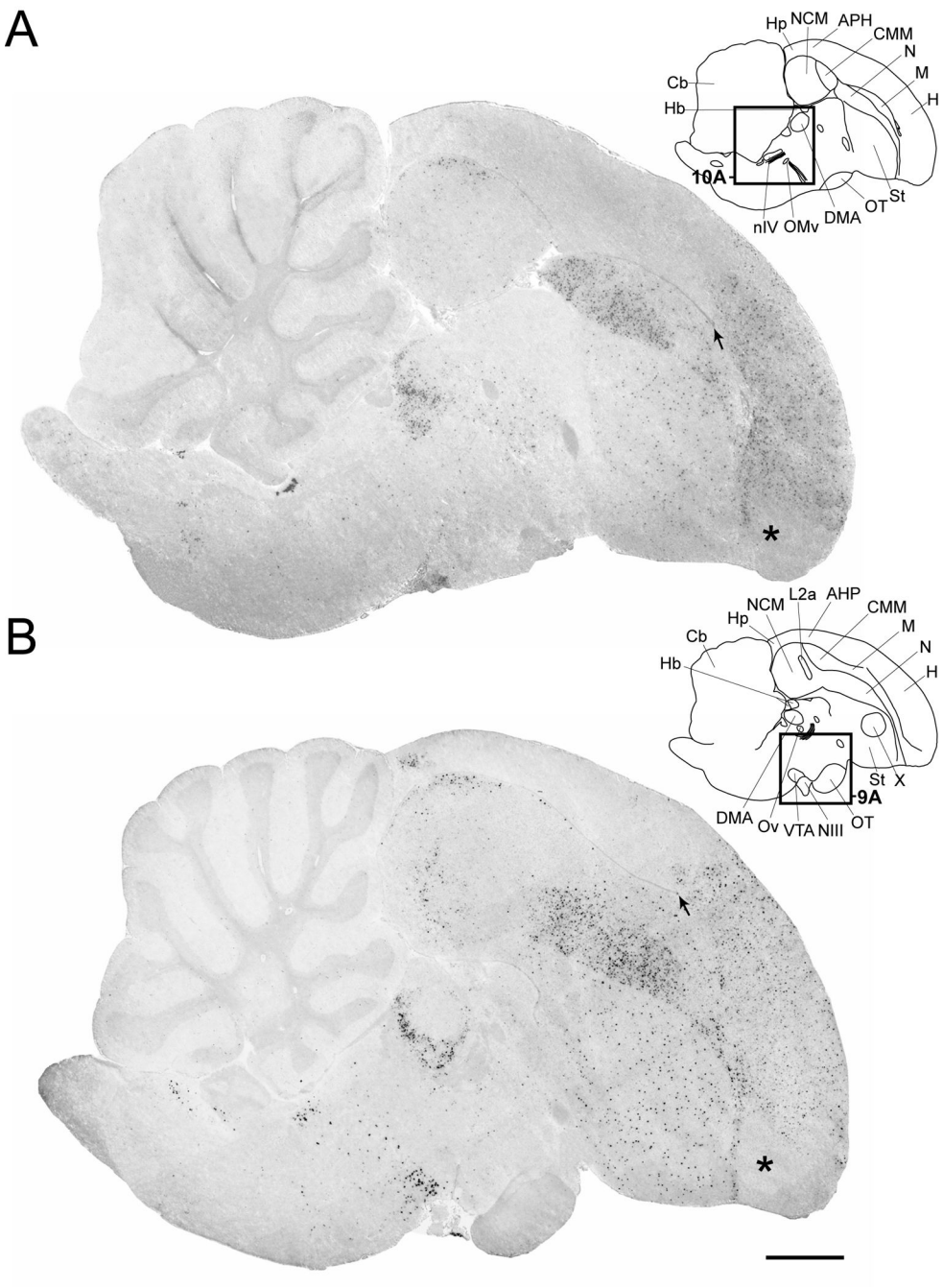

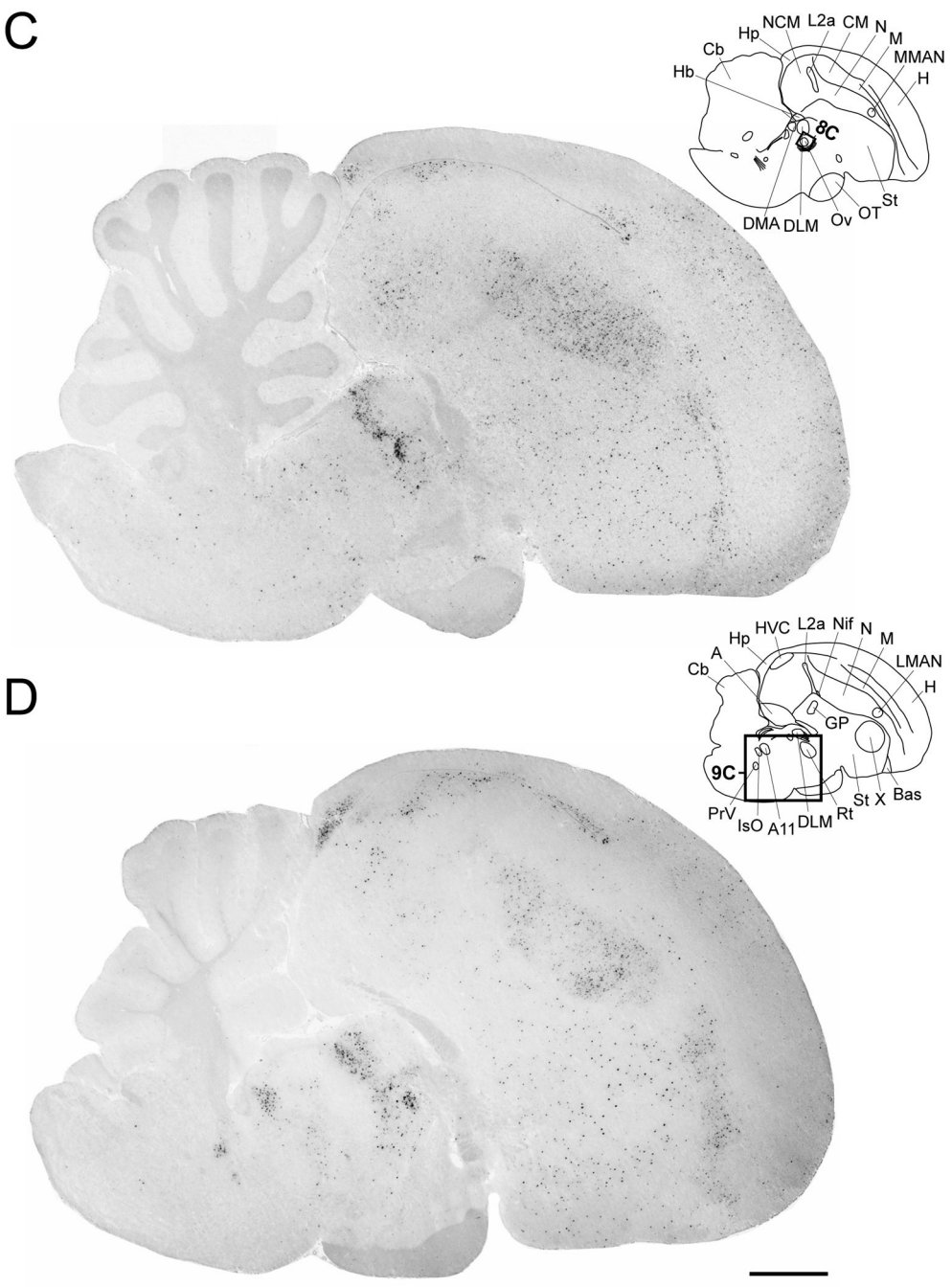

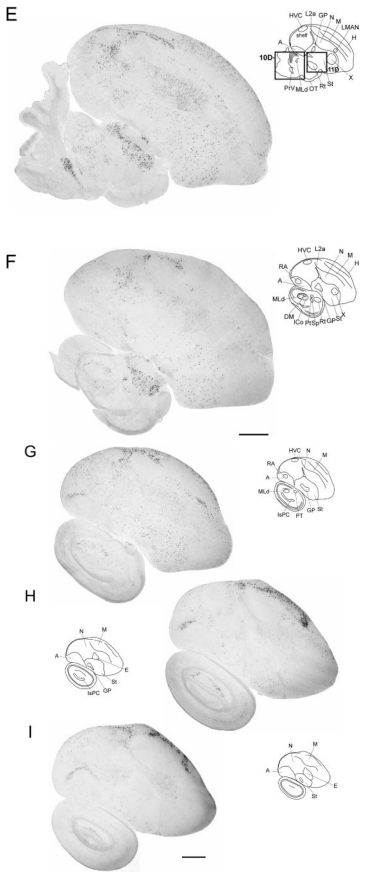

Figure 4.

Cck expression in serial parasagittal sections from an adult male zebra finch brain. Left panels in **A–I** are high-resolution photo-montaged images of *in situ* hybridization data in sections ~0.2 mm (**A**), ~0.6 mm (**B**), ~1.0 mm (**C**), ~1.4 mm (**D**), ~1.8 mm (**E**), ~2.2 mm (**F**), ~2.6 mm (**G**), ~3.2 mm (**H**), and ~3.6 mm (**I**) from the midline. The upper right panels in A–I are camera lucida drawings based on dark-field views of the sections shown in the left panels and superposition of cytoarchitectonic features seen on adjacent Nissl-stained sections. Rectangles in A–E indicate the relative positions of the drawing presented in Figures 8–11. Arrows in A and B denote the rostral tip of the lateral ventricle; asterisks in A and B indicate the possible location of an anterior olfactory area based on a comparison with the chick brain atlas. For anatomical abbreviations see Table 1. Scale bar: 1mm.

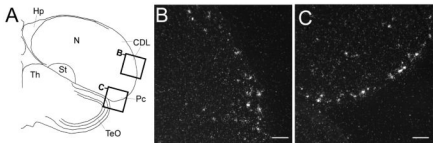

Figure 5.

Cck expression in the dorsolateral corticoid area and the piriform cortex. (**A**) Camera lucida drawing of a frontal section at the level of the caudal thalamus and hippocampus. Rectangles depict the locations of the photomicrographs shown in B and C. (**B, C**) High magnification dark-field views of emulsion autoradiography depicting *Cck*-labeled cells along the dorsolateral and ventrolateral telencephalon from the section depicted in (A). Based on a comparative analysis with the chick and pigeon brain atlases, these areas likely correspond to the external portion of the dorsolateral corticoid area (B) and the piriform cortex (C). Scale bars: 100 μm. For abbreviations see Table 1.

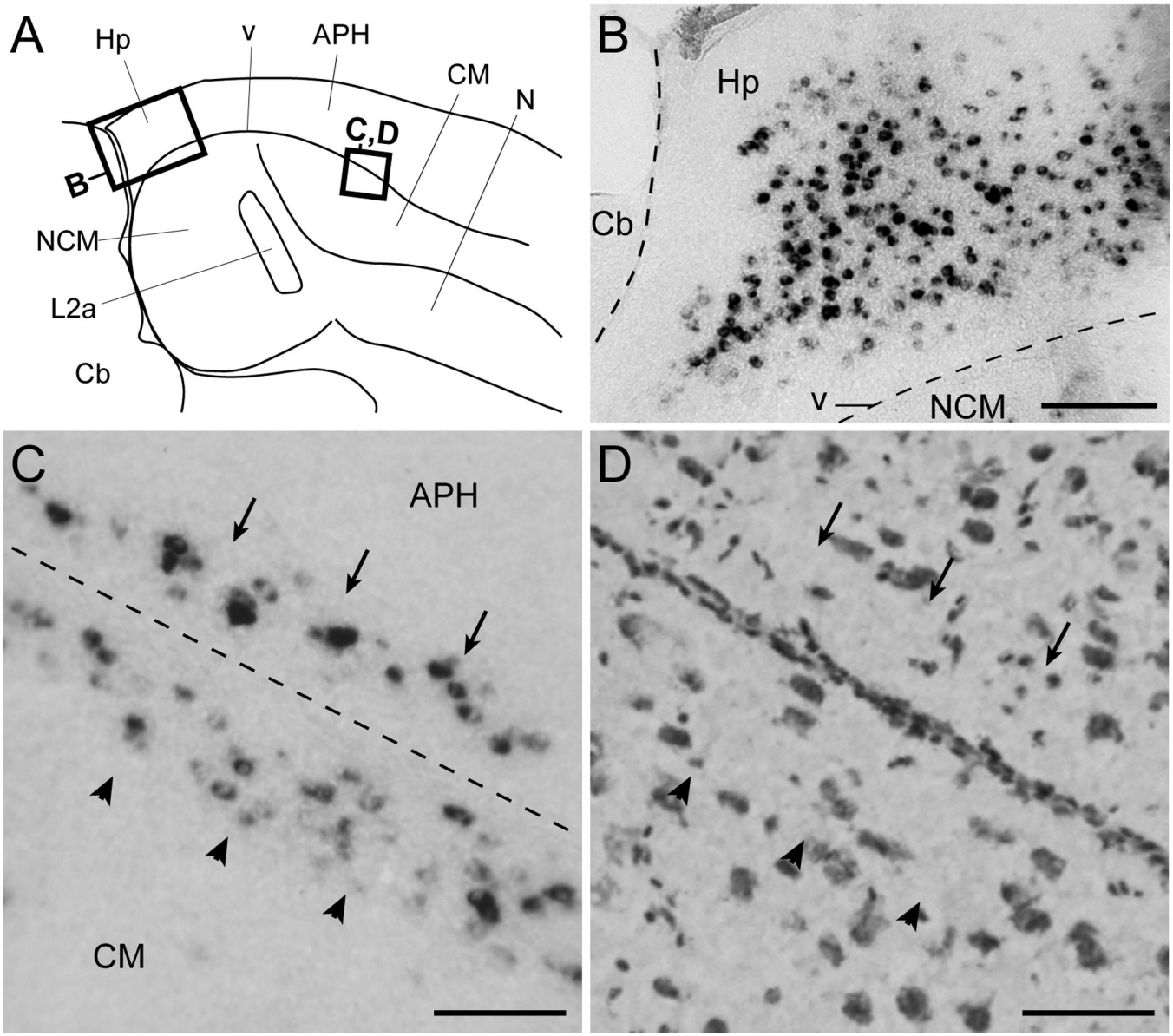

Figure 6.

Cck expression in the hippocampal formation and periventricular stratum. (**A**) Camera lucida drawing of a parasagittal section depicting the caudomedial auditory telencephalon and hippocampal formation (location indicated in Fig. 1A). Rectangles indicate the location of the photomicrographs in B–D. (**B**) Detail view of *Cck*-labeled cells within the hippocampal formation in a parasagittal brain section; the dashed lines indicate the location of the ventricle and pial surface between the cerebellum and NCM. (**C**) Detail view of labeled cells along a narrow periventricular band beneath the ventral-most region of the parahippocampal area (APH, arrows) and the dorsal portion of the caudal mesopallium (CM, arrowheads); he approximate location of the ventricle is depicted by the dashed line. (**D**) Bright-field view of Nissl-stained cells in a parasagittal section immediately adjacent to that shown in C; arrows and arrowheads are at the same relative positions as the ones in C. Scale bars: 200 μm for B; 100 μm for C–D; For abbreviations see Table 1.

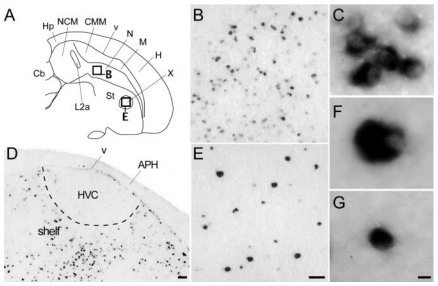

Figure 7.

Cck expression in nidopallial and sub-pallial areas. (**A**) Camera lucida drawing of a parasagittal section through the telencephalon (similar level as in Fig. 4B). Rectangles indicate the locations of the photomicrographs in B and E. (**B–G**) Bright-field views of *Cck* positive cells within various portions of the nidopallium, and striatum in a parasagittal section. (B) Low power view of populations of *Cck*-expressing cells with high labeling intensity interspersed among cells with low intensity labeling in the medial intermediate nidopallium. (**C**) High power view of a cluster of small, round cells with high labeling intensity within the intermediate nidopallium. (**D**) High magnification view of labeled cells laterally within the nidopallial auditory shelf region ventral to HVC (location indicated in Fig. 4E); note cells are mostly absent within HVC. (**E**) Low magnification view of interspersed large and small cells with high labeling intensity within striatal song nucleus area X. Image was taken at the same magnification as the photomicrograph in B. (**F–G**) High magnification views of strongly-labeled small (F) and large (G) cells in area X. Scale bars: 100 μm for B and E, 100 μm for D, and 10 μm for C, F and G. For abbreviations see Table 1.

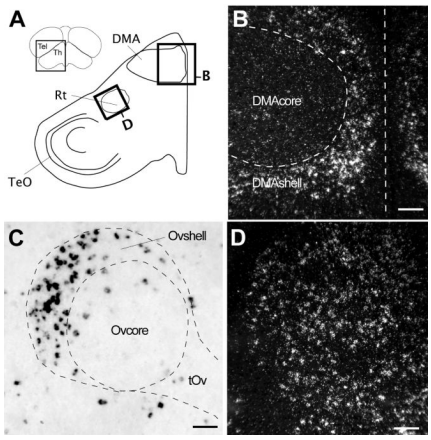

Figure 8.

Cck expression in the thalamus. (**A**) Camera lucida drawing of a frontal section depicting some major nuclei in the thalamus (location indicated in the section on the top left inset). Rectangles denote the locations of the photomicrographs in B and D. (**B**) Dark-field view in a frontal section of emulsion autoradiography showing *Cck* expression restricted to the shell of DMA. Dashed lines denote the approximate boundary of the DMA core based on Nissl staining and define the midline. (**C**) High power bright-field view from a parasagittal section through the thalamus (location indicated in Fig. 4C) showing labeled cells within the shell of nucleus ovoidalis (Ov). The dotted lines denote the approximate boundaries of the Ovcore/Ovshell and tract (tOv), based on Nissl staining. (**D**) Dark-field view in a frontal section of emulsion autoradiography depicting *Cck* expression in nucleus rotundus (Rt). Scale bars: 100 μm. For other abbreviations see Table 1.

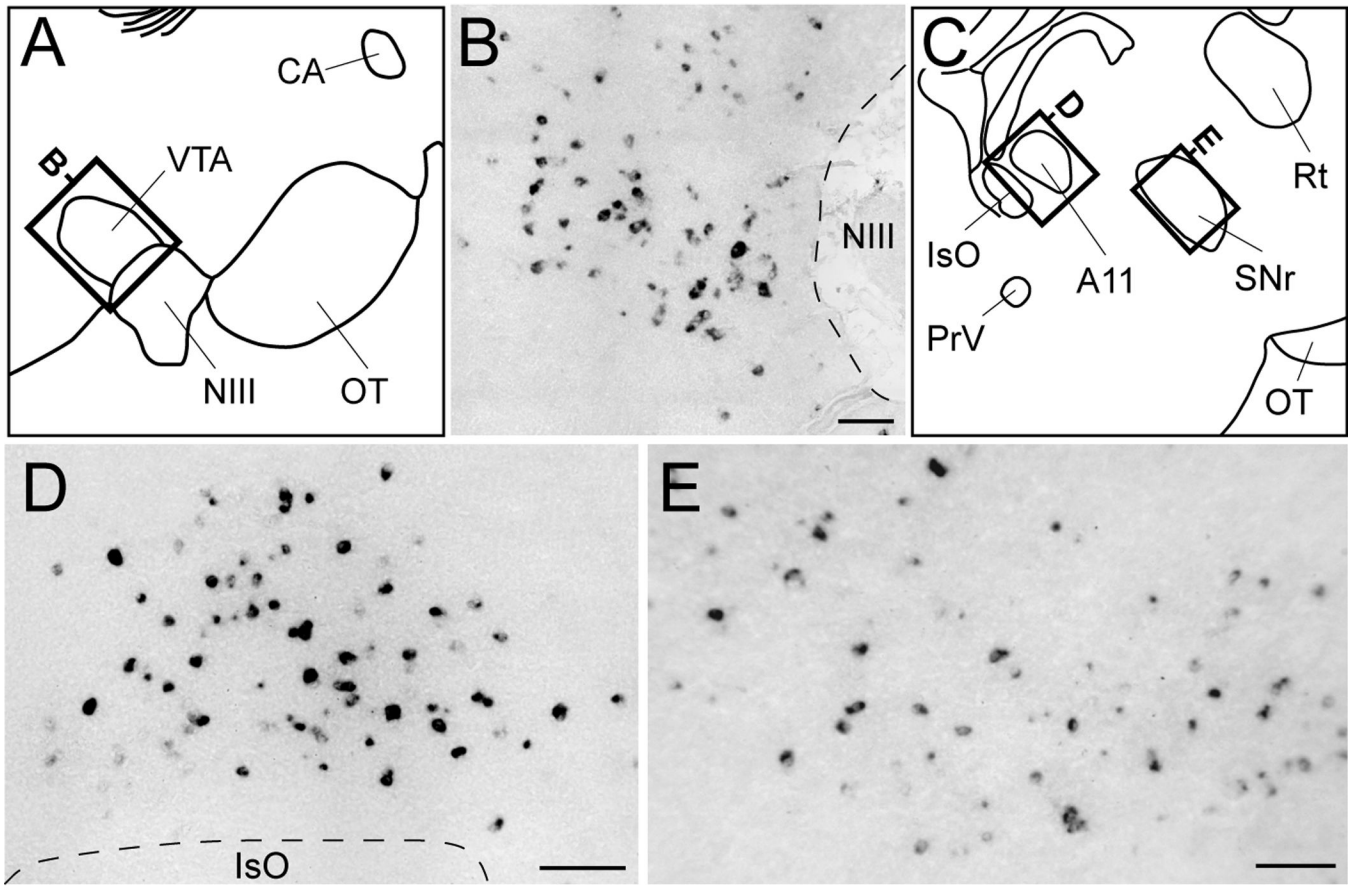

Figure 9.

Cck expression within midbrain dopaminergic nuclei. (**A**, **C**) Camera lucida drawings from a sagittal brain section depicting dopaminergic cell groups in the midbrain (locations indicated in Fig. 4B and D, respectively). Rectangles indicate the location of the photomicrographs shown in B and D–E. (**B**, **D–E**) High magnification bright-field views depicting *Cck*-labeled cells in the ventral tegmental area (VTA; **B**), dopaminergic cell group A11 (**D**), and substantia nigra pars reticulata (SNr; **E**). Dashed lines depict the boundaries of oculomotor nucleus fibers (**B**) and of IsO (**D**). Scale bars: 100 μm. For other abbreviations see Table 1.

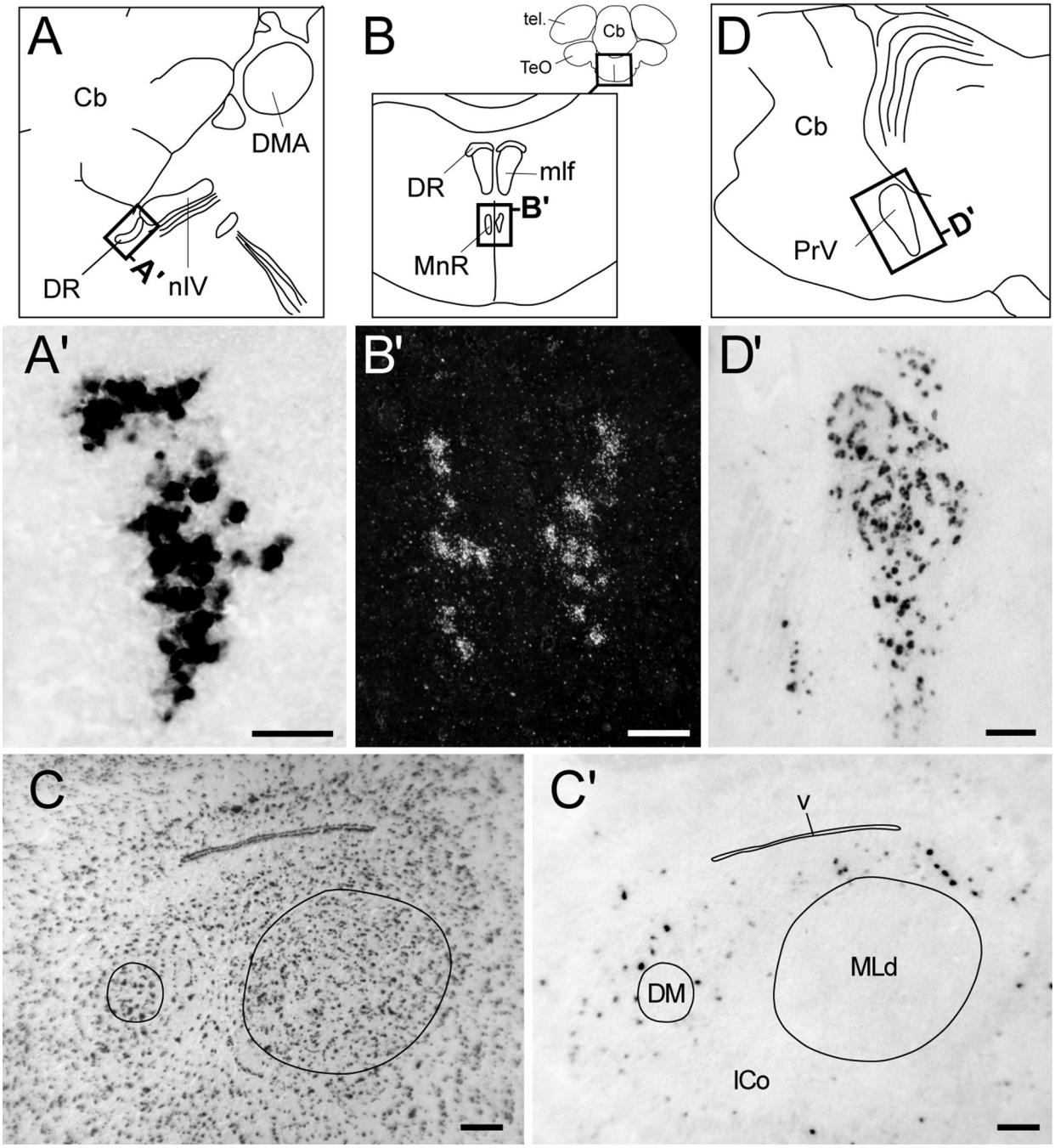

Figure 10.

Cck expression in mesencephalic and metencephalic nuclei. (**A, B**) Camera lucida drawings of the midbrain from a parasagittal section (**A**, location indicated in Fig. 4A), a frontal section (**B**, location indicated by rectangle in the upper right inset). Rectangles indicate the locations of the photomicrographs shown in A' and B'. (**A'**) Bright-field view in a frontal section of *Cck*-labeled cells in the dorsal raphe (DR). (**B'**) Dark-field view of emulsion autoradiography showing labeled cells within the median raphe nucleus (MnR). (**C, C'**) Low power bright-field views of parasagittal sections through the midbrain's intercollicular complex (ICo) in adjacent Nissl-stained (**C**) and chromagen-reacted sections (**C'**) showing sparse *Cck*-labeled cells within shell-like regions outside of nuclei MLd and DM, but not

within the core regions of these nuclei (core boundaries indicated by solid lines). (**D**) Camera lucida drawing of the pons from a parasagittal section (location indicated in Fig. 4E). Rectangle indicates the location of the photomicrograph shown in D'. (**D'**) Bright-field view of *Cck*-labeled cells in the principal trigeminal nerve nucleus (PrV). Scale bars: 100 μm. For abbreviations see Table 1.

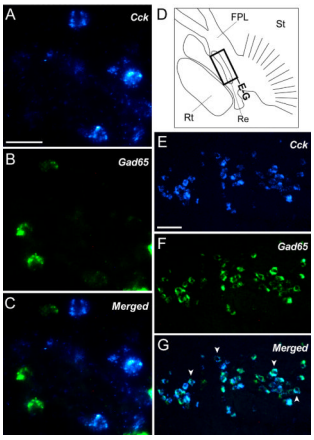

Figure 11.

Cck-expressing cells are non-GABAergic. (**A–C**) High power views of the nidopallium in a parasagittal section depicting *Cck*-positive cells (A; blue channel), *Gad65*-positive cells (B; green channel), and a merge of the two channels (C). Cell nuclei in A and B (red channel) were revealed by propidium iodide. (**D**) Camera lucida drawing of a parasagittal section (similar level as in Fig. 4E) showing detailed view of the thalamus and basal forebrain. Rectangle indicates the location of the photomicrographs shown in E–F. (**E–G**) Low power views of the reticular nucleus of the thalamus (Re) depicting *Cck*-labeled cells (E; blue channel), *Gad65*-positive cells (F; green channel), and a merge of the two channels (G). Arrowheads in G indicate examples of double-labeled cells. Scale bars: 10 μm for A-C; 100 μm for E–G. For abbreviations see Table 1.

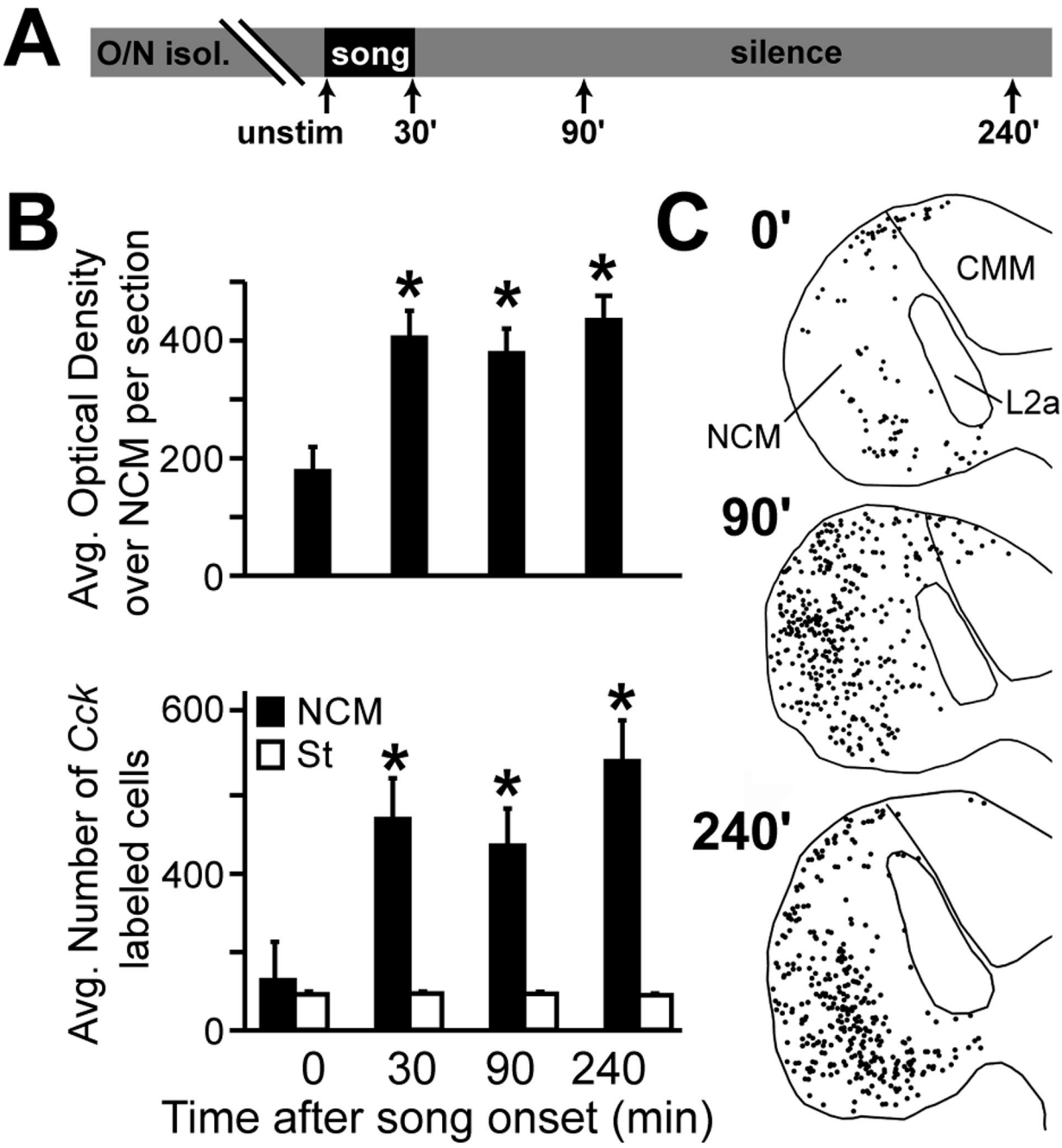

Figure 12.

Song stimulation induces *Cck* expression in NCM. (**A**) Schematic showing the design of the song stimulation experiment (see Materials and Methods for details); arrows indicate the time (in minutes) that females were sacrificed following the onset of song stimulation (see Materials and Methods for details). (**B**) Average optical density values from phosphorimager autoradiography representing *Cck* expression over NCM (top panel), and counts of *Cck*-expressing cells within NCM (bottom panel; black bars) and the striatum (white bars) measured 0, 30, 90, and 240 minutes after song stimulation onset. Asterisks denote values that were significantly different from the unstimulated control group (time 0) according to an ANOVA and *post hoc* t-tests. (**C**) Representative maps (from parasagittal sections at ~0.6

mm from the midline) showing *Cck*-expressing cells (black circles) that were detected in NCM by fluorescent *in situ* hybridization 0, 90, and 240 minutes after the onset of song stimulation.

Table 1

Abbreviations

A	arcopallium
A11	All dopaminergic cell group
APH	area parahippocampalis
Bas	nucleus basorostralis
CA	anterior commissure
CDL	area corticoidea dorsolateralis
CM	caudal mesopallium
CMM	caudomedial mesopallium
DLM	medial part of the dorsolateral nucleus of thalamus
DM	dorsal medial nucleus of the ICo
DMA	dorsomedial nucleus of the anterior thalamus
DR	dorsal raphae nuclei
E	entopallium
FPL	fasciculus prosencephali lateralis
GP	globus pallidus
H	hyperpallium
Hb	habenula
HP	hippocampus
HVC	HVC(as proper name)
ICo	nucleus intercollicularis
IsPC	nucleus isthmi, pars parvocellularis
IsO	nucleus isthmo-opticus
L2a	subfield L2a of field L
LMAN	lateral magnocellular nucleus of the anterior nidopallium
M	mesopallium
MLd	nucleus mesencephalicus lateralis, pars dorsalis
mlf	medial longitudinal fascicle
MMAN	medial magnocellular nucleus of the anterior nidopallium
MnR	median Raphe nucleus
N	nidopallium
NCM	caudomedial nidopallium
Nif	nucleus interfacialis
NIII	oculomotor nerve
nIV	nucleus of the trochlear nerve
OMv	ventral part of the oculomotor nerve nucleus
OT	optic tract
Ovcore	nucleus ovoidallis(core)
Ovshell	nucleus ovoidallis(shell)
PC	piriform cortex
PrV	principal trigeminal nerve nucleus

PT	nuclus pretectalis
RA	robust nucleus of the arcopallium
Re	reticular nucleus of the thalamus
Rt	nucleus rotundus
SNr	substantia nigra pars reticularis
Sp	nucleus spiriformis
St	striatum
V	optic tectum
TeO	ventricle
X	area X
Tel	telencephalon
Th	thalamus
tOv	tractus ovoidalis
VTA	ventral tegmental area

TABLE 2

Relative Expression Levels[1] of *Cck* in the Zebra finch Brain[2]

Telencephalon		**Dlencephalon**	
Hippocampal formation	+	Thalamus	++
Hp (caudal)	+++	DMAcore	−
APH	−	DMAshell	++++
Hyperpallium	+++	DLMcore	−
CDL	++++	DLMshell	++++
Piriform cortex	++++	Ovcore	−
Anterior olfactory area	−	Ovshell	++++
Periventricular stratum	++	Rt	++++
Mesopallium	+	Re	+++
CMM	−	Hb	−
Nidopallium	++	Hypot halamus	−
NCM	+		
Intermediate part	++++	**Mesencephalon**	
Rostral part	+++	PT	−
shelf	++++	Sp	−
MMAN/LMAN	−	TeO	−
HVC	−	Ico	++
Nif	−	MLd	−
L2a	−	DM	−
Bas	−	DR	++++
E	−	MnR	++++
Arcopallium	+	VTA	+++
Dorsal arcopallium	+++	SNr	++
RA	−		
TnA	−	**Metencephalon**	
Striatum (St)	++	Pons	++
Area X	++	A11	++
GP	−	PrV	++++
Septum	−		

[1] Semi-quantitative scale based on a visual inspection of signal density.

[2] For abbreviations see Table 1.